Electronic Supplementary Information (ESI)

Annulated oxazolium salts as anion-π^+ interaction-enabled solid-state room-temperature phosphorescent materials

Shivankar Jagota,[$a] Samim Sohel Rana,[$a] Chhotan Barman[a] and Joyanta Choudhury[*a]

[a]Organometallics & Smart Materials Laboratory, Department of Chemistry
Indian Institute of Science Education and Research Bhopal
Bhopal 462 066, India
E-mail: joyanta@iiserb.ac.in

[$] These authors contributed equally.

Table of contents

1. General methods and materials

Bruker AVANCE III 400 MHz, 500 MHz, and 700 MHz NMR spectrometers were used to record ^{1}H, and ^{13}C{^{1}H} spectra at room temperature unless otherwise indicated. Chemical shifts are represented in parts ppm using the solvents residual proton resonance as an internal reference (CH_3CN: 1.94 ppm for ^{1}H NMR spectra, 1.3, 118.2 ppm for ^{13}C{^{1}H} NMR spectra). Unless otherwise specified, all coupling constants (*J*) are reported in hertz (Hz) and are exclusively given for ^{1}H-^{1}H couplings. To signify multiplicity, the following acronyms were used: s (singlet), d (doublet), dd (doublet of doublets), m (multiplet). A Bruker microTOF QII instrument was used for ESI mass spectrometry. The products were purified chromatographically using column chromatography on silica gel (230-400 mesh). Single-crystal X-ray diffraction data were collected at low temperature (140 K) using a Bruker D8 QUEST PHOTON 100 diffractometer equipped with graphite-monochromated Mo Kα radiation (λ = 0.71073 Å). Data reduction was performed using the Bruker Apex V software suite, and the crystal structures were solved via Intrinsic Phasing using the ShelXT program. The solution-state UV-visible absorption spectra were obtained using a Cary 100 UV-Vis spectrophotometer at room temperature, and solid-state spectra were obtained using Shimadzu UV-2600I spectrophotometer, while steady-state fluorescence measurements were conducted using a HORIBA Fluoromax spectrofluorometer. Time-resolved fluorescence spectroscopy was performed with a FLS1000 spectrometer, Edinburgh Instruments, and Delta Flex-01 DD/HORIBA. Phosphorescence spectra were obtained using a HORIBA Fluorolog spectrofluorometer. Powder XRD patterns were obtained using PANalytical Empyrean X-ray Diffractometer.

Dry solvents and reagents were purchased from commercial suppliers and used without further purification. Deuterated solvents and $RhCl_3.xH_2O$ were purchased from Aldrich. $[RhCp^*Cl_2]_2$ was synthesized according to the reported procedure.[S1]

2. General procedure for the catalytic annulation reactions

In a Schlenk tube, oxazolium salt (0.1 mmol), NaOAc (4.2 equiv.), $[RhCp^*Cl_2]_2$ (1.8 mg, 3 mol%), AgOTf (64.3 mg, 0.25 mmol), and alkyne (0.12 mmol) were loaded. Then the system was evacuated for 5 minutes to remove any residual air or moisture and filled with N_2 gas. Subsequently, dry and degassed dichloroethane (DCE, 2.0 mL) was added to the mixture, and the reaction was carried out at 110 °C for 24 hours in the dark. The reaction mixture was subsequently passed through a short column of celite and washed with dichloromethane (DCM, 30 mL). The combined filtrate was concentrated under reduced pressure, and the final product was isolated using column chromatography eluting with a mixture of dichloromethane and methanol (2% DCM/MeOH).

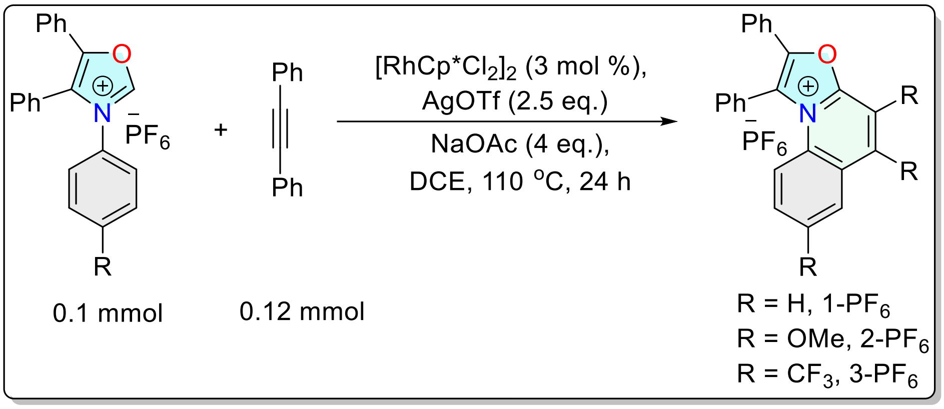

Scheme S1. Synthesis of the annulated oxazolium compounds

3. General procedure for reversible counter-anion exchange

In a 25 mL round-bottom flask, oxazolium salt (0.1 mmol) was dissolved in 2 mL of MeOH under an inert atmosphere. To this solution, an excess amount of tetrabutylammonium iodide (TBAI) was added with continuous stirring. The mixture was stirred at room temperature for 2 h. The resulting precipitate was collected by filtration and washed several times with diethyl ether and hexane, then dried under vacuum to yield the product as a yellow coloured solid. Further, potassium hexafluorophosphate (KPF_6) was added to the acetonitrile, water combination (1:1) of compounds containing iodide counter anion and stirred for two hours in order to exchange iodide with hexafluorophosphate. After washing with water and diethyl ether, the solid is dried under high vacuum to produce an off-white solid with hexafluorophosphate as counter anion.

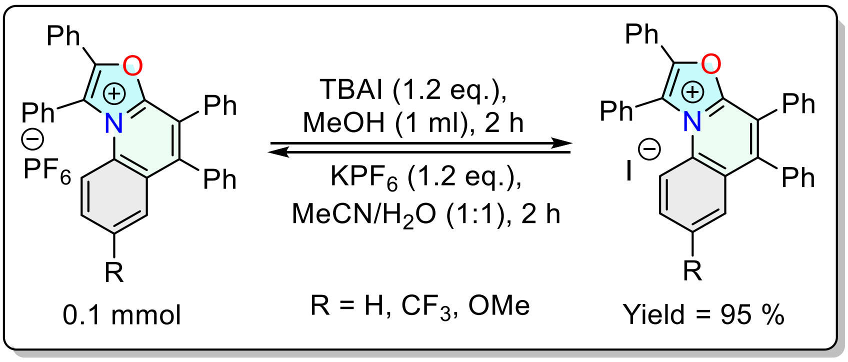

Scheme S2. Reversible counter-anion exchange

4. Experimental characterization data of 1-I, 2-I, 3-I

1,2,4,5-tetraphenyloxazolo[3,2-a]quinolin-10-ium iodide (1-I): Yield = 95 %, 57 mg, **^{1}H NMR** (500 MHz, CD_3CN) δ 7.96 – 7.82 (m, 3H), 7.74 (m, 1H), 7.50 (m, 5H), 7.41 (d, J = 3.5 Hz, 2H), 7.35 (d, J = 4.8 Hz, 1H). **^{13}C NMR** (700 MHz, CD_3CN) δ 153.8, 153.5, 150.7, 134.6, 133.8, 132.8, 132.3, 132.1, 131.3, 131.1, 131.0, 130.8, 130.7, 130.6, 130.5, 130.4, 129.8, 129.7, 128.3, 127.9, 127.6, 126.5, 125.3, 124.9, 124.8, 124.6, 123.3. **HRMS** (ESI, positive ion): M^+ = 474.1844 (calculated 474.1853 for $[C_{35}H_{24}NO]^+$).

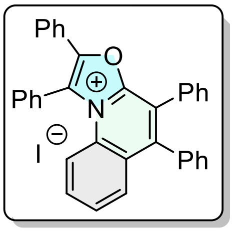

7-methoxy-1,2,4,5-tetraphenyloxazolo[3,2-a]quinolin-10-ium iodide (2-I) : Yield = 95%, 60 mg, **^{1}H NMR** (500 MHz, CD_3CN) δ 7.92 – 7.83 (m, 5H), 7.48 (dd, J = 2.5 Hz, 1H), 7.47 – 7.38 (m, 12H), 7.37 – 7.30 (m, 5H), 7.15 (d, J = 2.9 Hz, 1H), 3.70 (s, 3H**)**. **^{13}C NMR** (700 MHz, CD_3CN) δ 159.9, 134.8, 133.5, 132.5, 132.4, 131.9, 131.5, 131.2, 130.9, 130.3, 129.6, 127.7, 126.0, 123.6, 111.0, 56.5. **HRMS** (ESI, positive ion): M^+ = 504.1949 (calculated 504.1959 for $[C_{36}H_{26}NO_2]^+$).

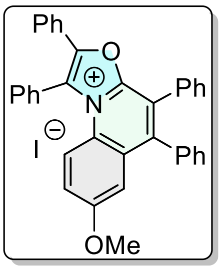

1,2,4,5-tetraphenyl-7-(trifluoromethyl)oxazolo[3,2-a]quinolin-10-ium iodide (3-I): Yield = 94%, 63 mg, **^{1}H NMR** (500 MHz, CD_3CN) δ 8.12 (s, 1H), 7.99 – 7.92 (m, 2H), 7.89 – 7.84 (m, 4H), 7.69 (d, J = 9.3 Hz, 1H), 7.54 – 7.47 (m, 9H), 7.43 – 7.40 (m, 4H), 7.39 – 7.34 (m, 2H). **^{13}C NMR** (700 MHz, CD_3CN) δ 153.8, 153.5, 150.6, 134.6, 133.8, 133.7, 132.8, 132.3, 132.0, 131.3, 131.1, 130.7, 130.6, 130.5, 130.3, 129.7, 129.7, 129.6, 128.3, 128.2, 127.8, 127.6, 126.5, 125.4, 124.9, 124.6, 119.7. **HRMS** (ESI, positive ion): M^+ = 542.1715 (calculated 542.1727 for $[C_{36}H_{23}F_3NO]^+$).

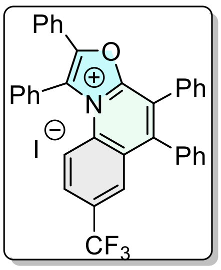

5. Spectral data of 1-I, 2-I, 3-I

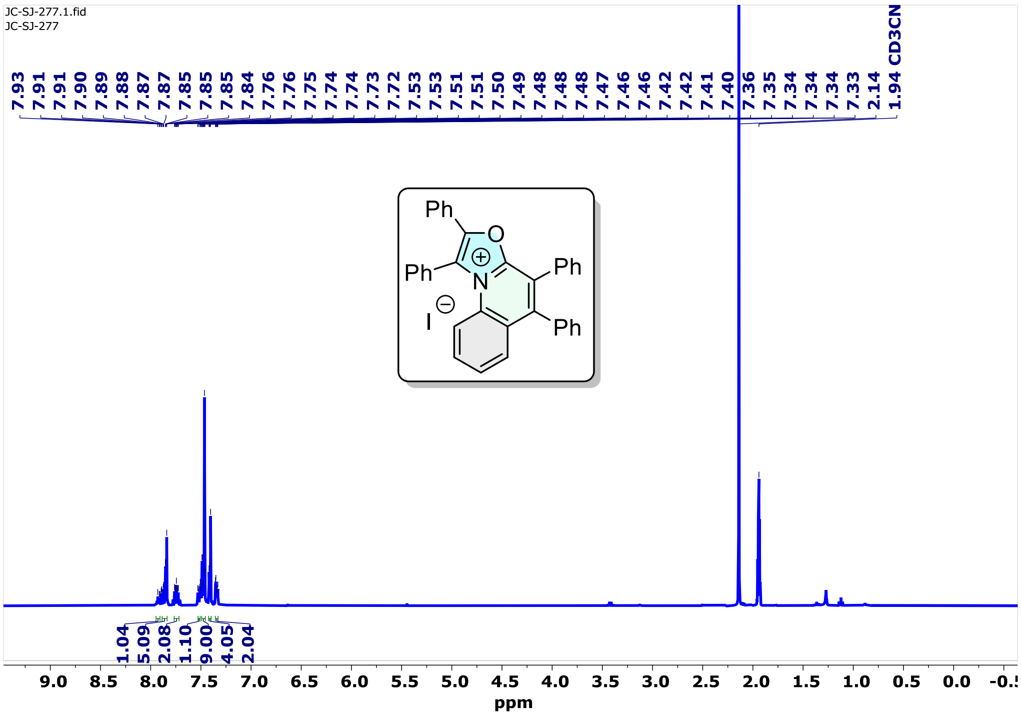

Figure S1. ^{1}H NMR spectrum of **1-I** (500 MHz, CD_3CN)

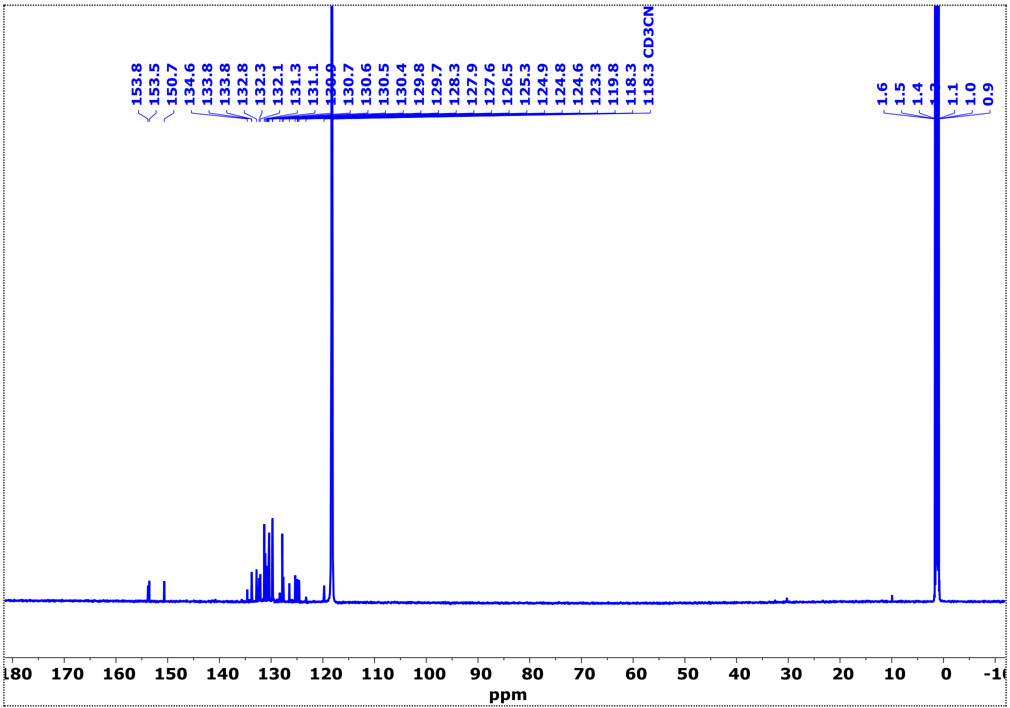

Figure S2. $^{13}C\{^{1}H\}$ NMR spectrum of **1-I** (176 MHz, CD_3CN)

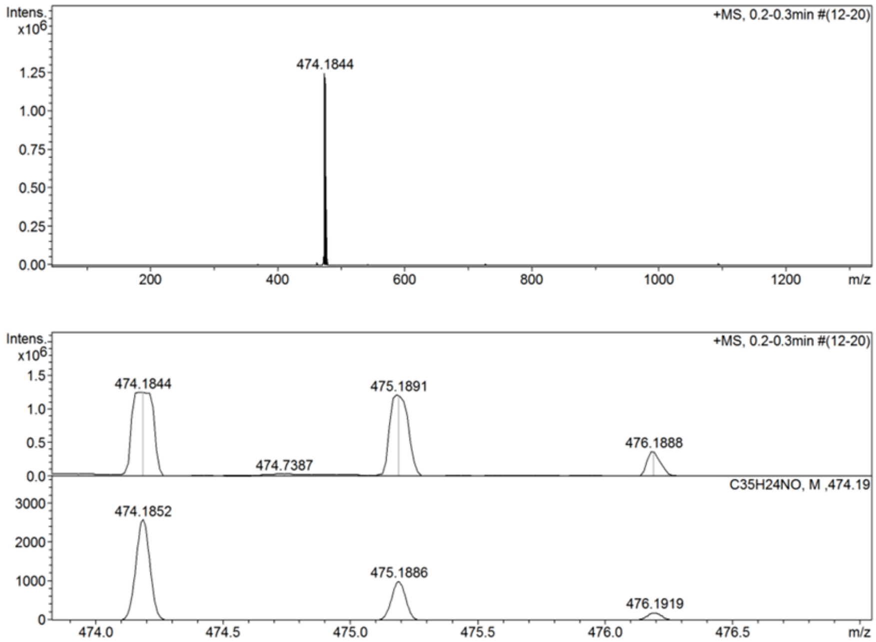

Figure S3. ESI-HRMS (positive ion mode) spectrum of **1-I**

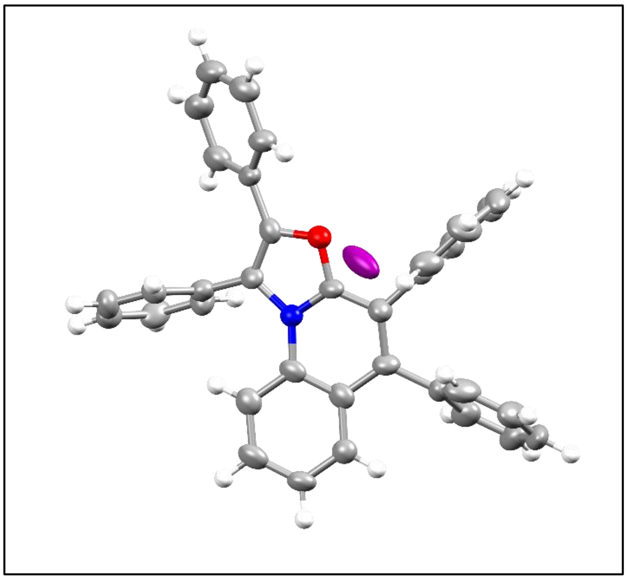

Figure S4. Molecular structure of **1-I** (50% probability level)

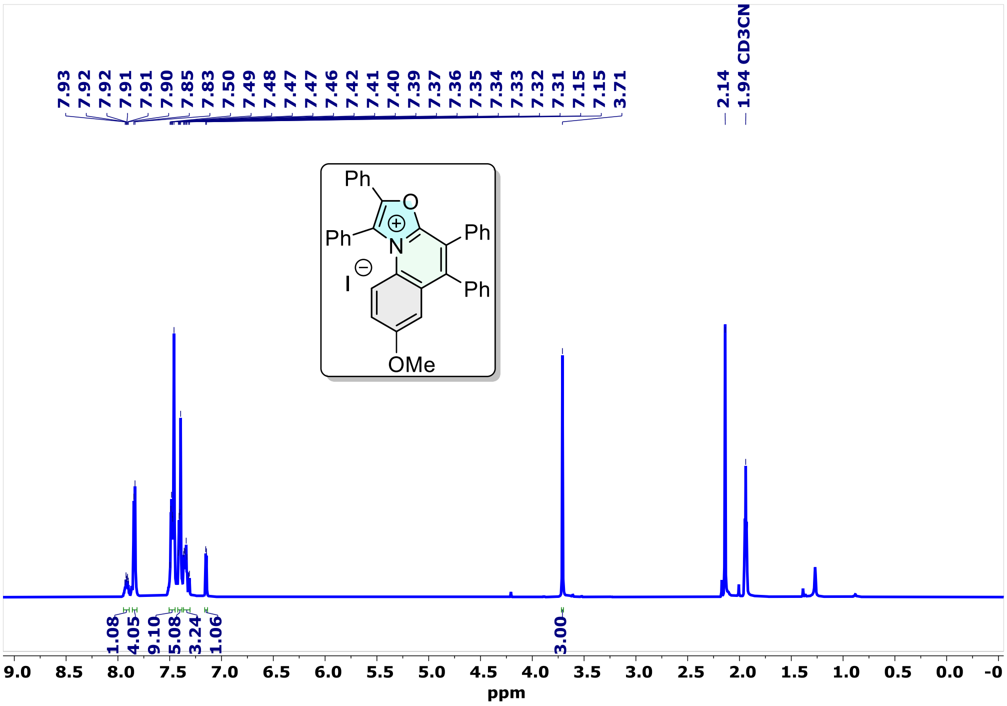

Figure S5. ^{1}H NMR spectrum of **2-I** (500 MHz, CD_3CN)

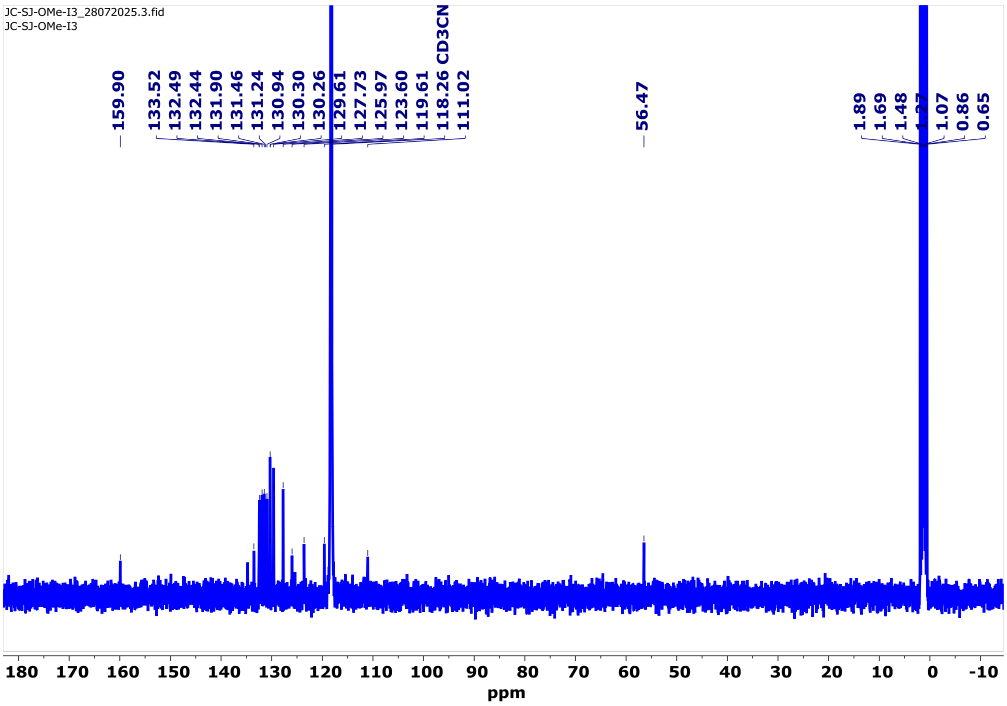

Figure S6. $^{13}C\{^{1}H\}$ NMR spectrum of **2-I** (176 MHz, CD_3CN)

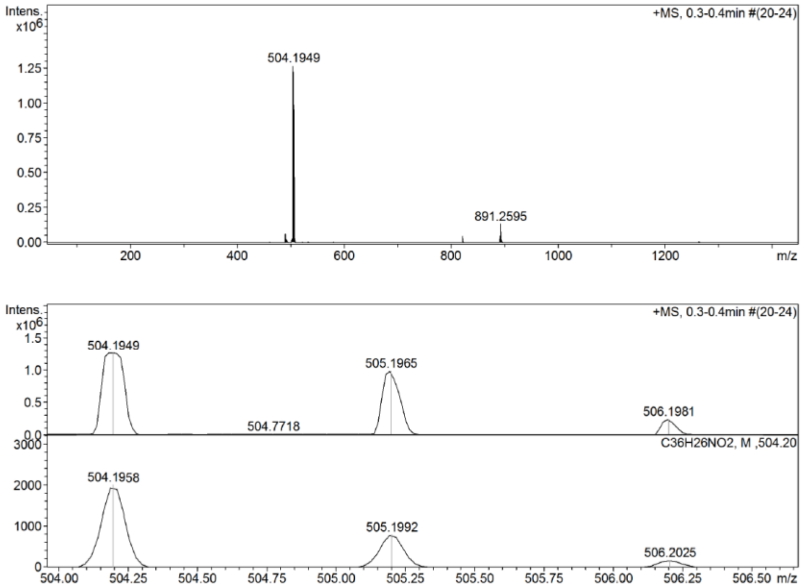

Figure S7. ESI-HRMS (positive ion mode) spectrum of **2-I**

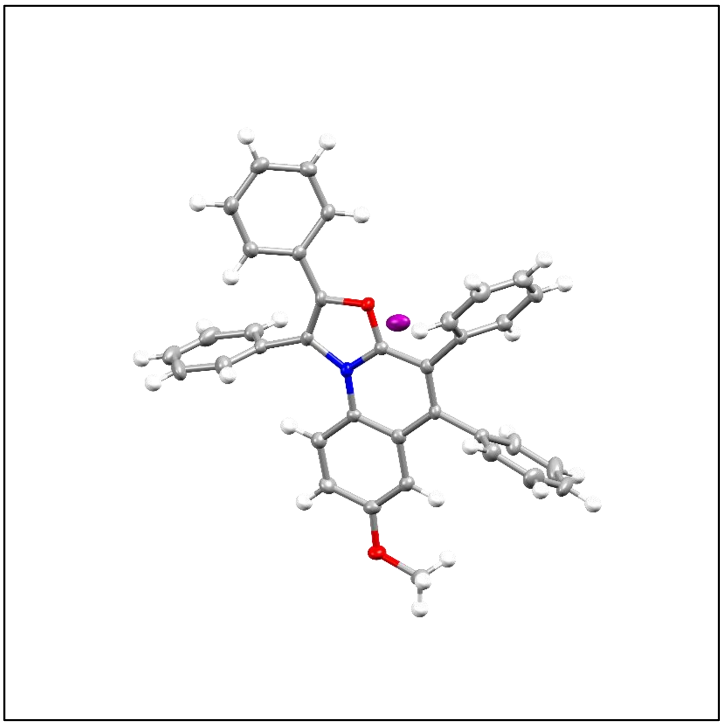

Figure S8. Molecular structure of **2-I** (50% probability level)

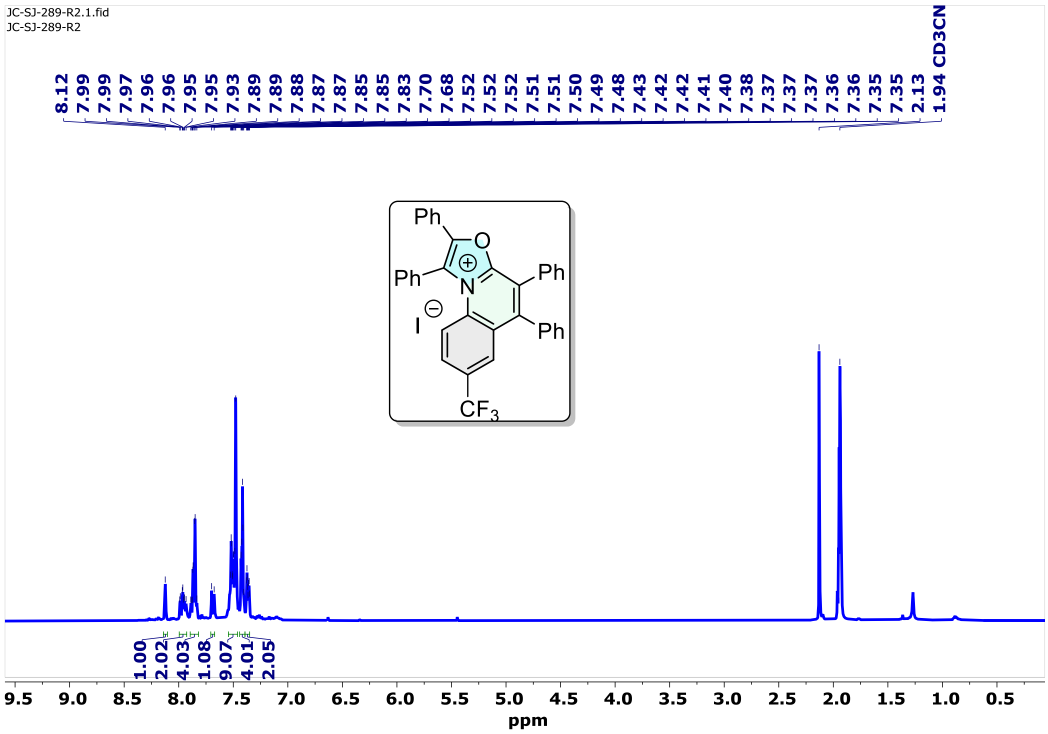

Figure S9. ^{1}H NMR spectrum of **3-I** (500 MHz, CD_3CN)

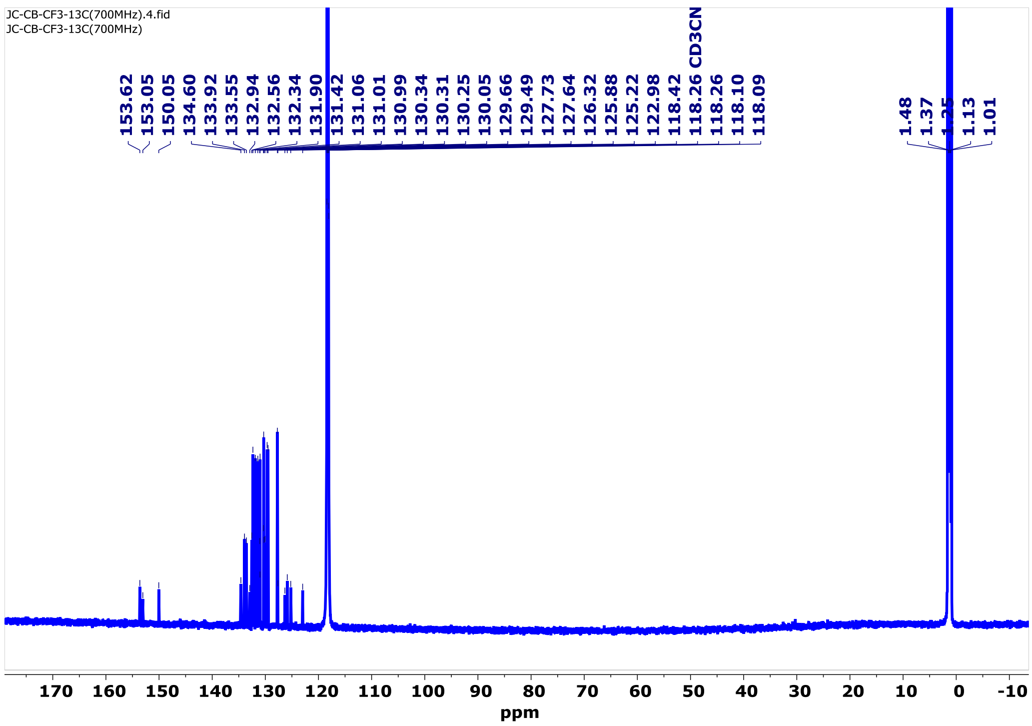

Figure S10. $^{13}C\{^1H\}$ NMR spectrum of **3-I** (176 MHz, CD_3CN)

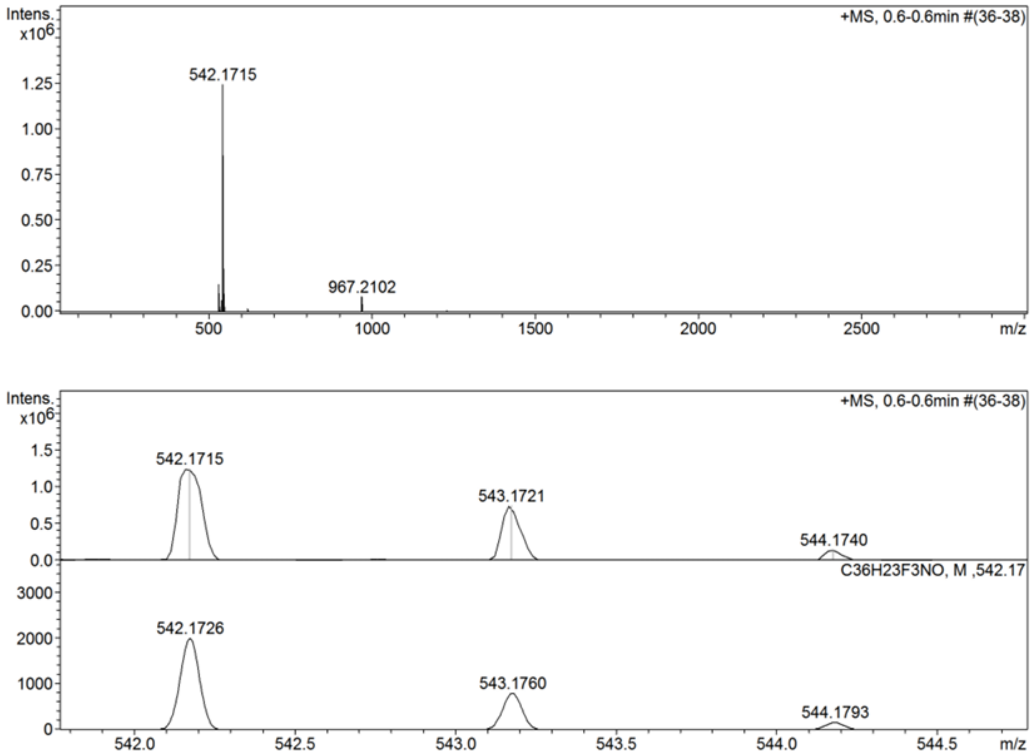

Figure S11. ESI-HRMS (positive ion mode) spectrum of **3-I**

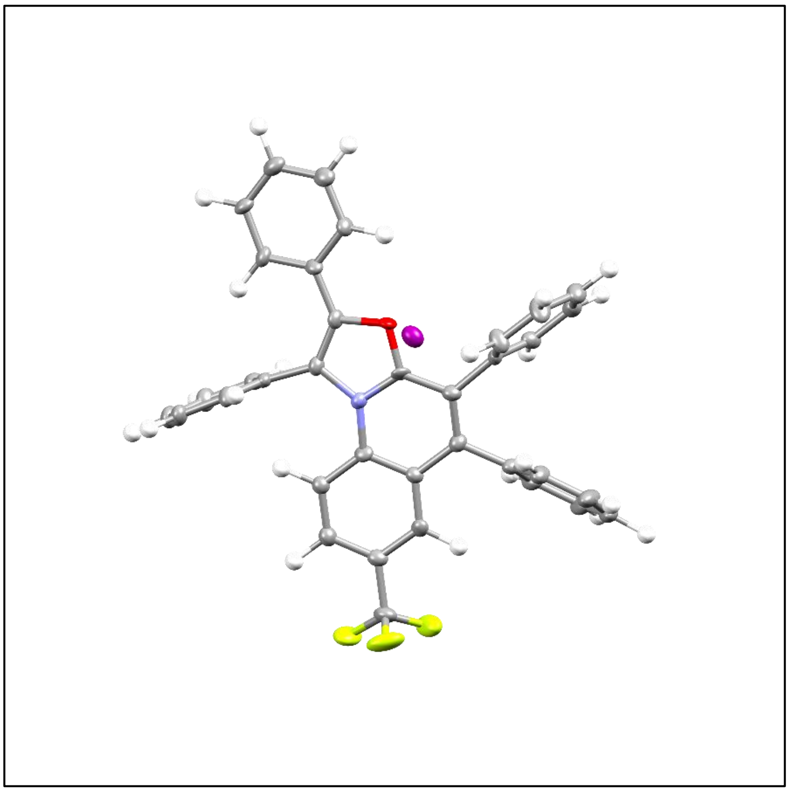

Figure S12. Molecular structure of **3-I** (50% probability level)

6. UV-visible and fluorescence/phosphorescence spectroscopic studies

The solution-state UV-visible absorption spectra were obtained using a Cary 100 UV-Vis spectrophotometer at room temperature (1.0 cm quartz cuvettes), and solid-state spectra were obtained using Shimadzu UV-2600I spectrophotometer, while steady-state fluorescence measurements were conducted using a HORIBA Fluoromax spectrofluorometer. Time-resolved fluorescence spectroscopy was performed with a FLS1000 spectrometer, Edinburgh Instruments, and Delta Flex-01 DD/HORIBA . Phosphorescence spectra were obtained using a HORIBA Fluorolog spectrofluorometer. Sample solutions of 1 mM were introduced into 2 mL dichloromethane solution, and the excitation wavelength was adjusted according to the sample to record the emission spectra.

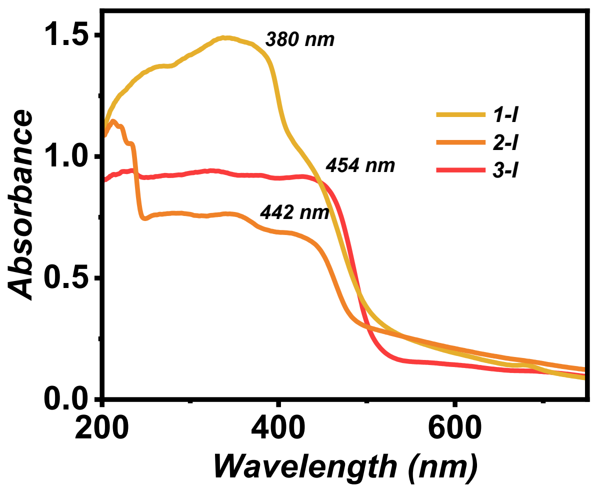

Figure S13. Solid-state UV-vis spectra of **1-I**, **2-I**, and **3-I**

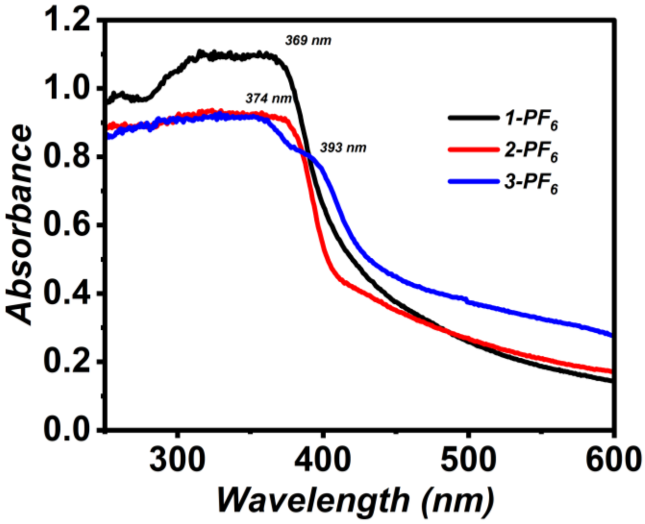

Figure S14. Solid-state UV-vis spectra of **1-PF$_6$**, **2-PF$_6$**, and **3-PF$_6$**

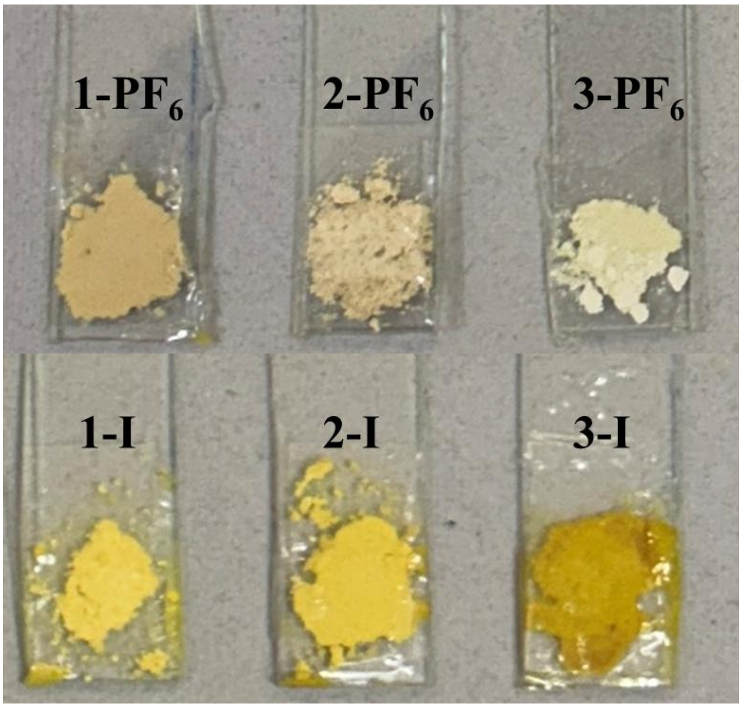

Figure S15. Photographs of the solid compounds **1-PF₆**, **2-PF₆**, **3-PF₆** and **1-I**, **2-I**, **3-I** under normal daylight

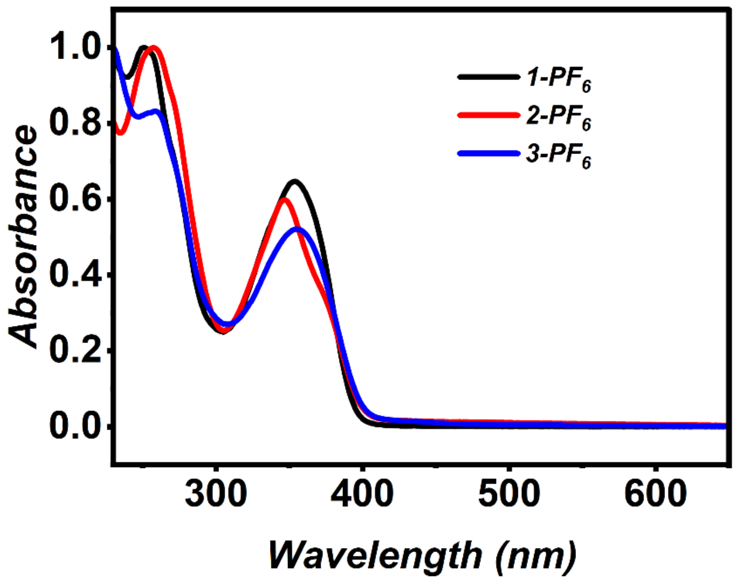

Figure S16. UV-vis spectra of **1-PF₆**, **2-PF₆**, **3-PF₆** in dichloromethane (25 μM)

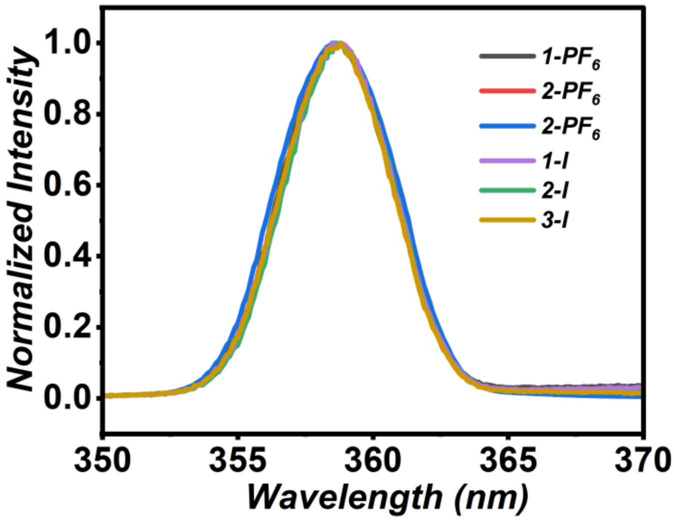

Figure S17. Excitation spectra of **1-PF₆**, **2-PF₆**, **3-PF₆**/ **1-I**, **2-I**, **3-I** in dichloromethane (25 μM)

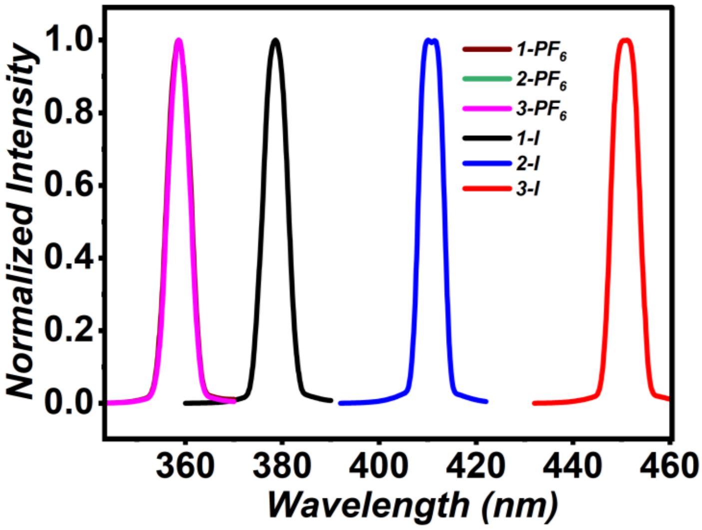

Figure S18. Excitation spectra of **1-PF₆**, **2-PF₆**, **3-PF₆**/ **1-I**, **2-I**, **3-I** in solid state

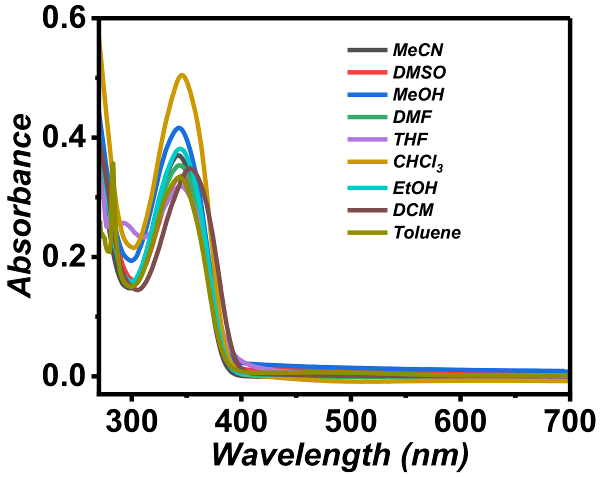

Figure S19. UV-vis spectra of **1-I** in different solvents (20 μM)

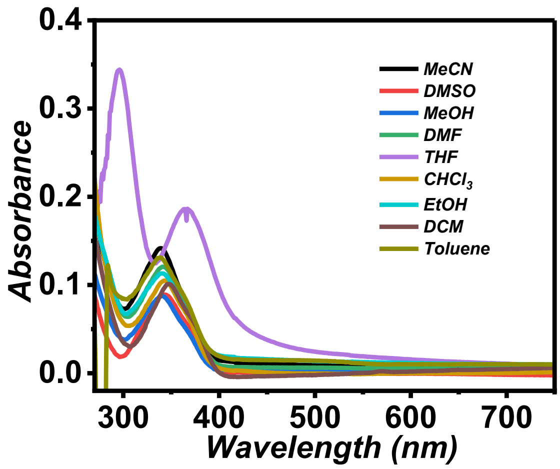

Figure S20. UV-vis spectra of **2-I** in different solvents (20 μM)

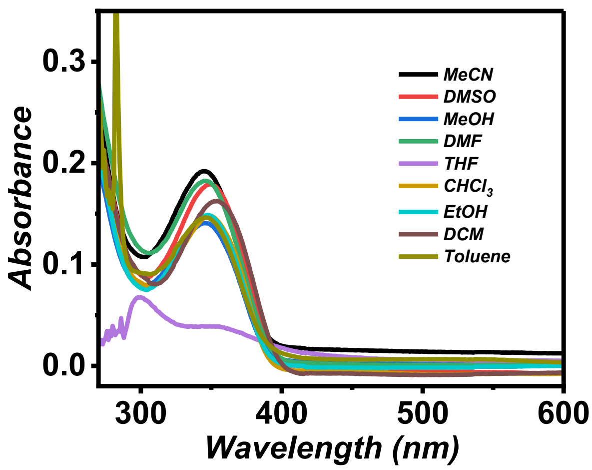

Figure S21. UV-vis spectra of **3-I** in different solvents (20 μM)

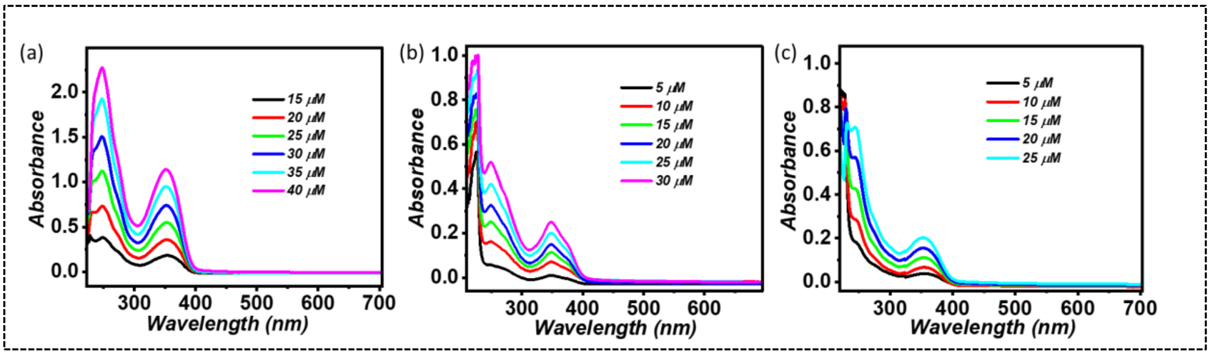

Figure S22. UV-vis spectra of (a) **1-I**, (b) **2-I**, (c) **3-I** at different concentrations in dichloromethane

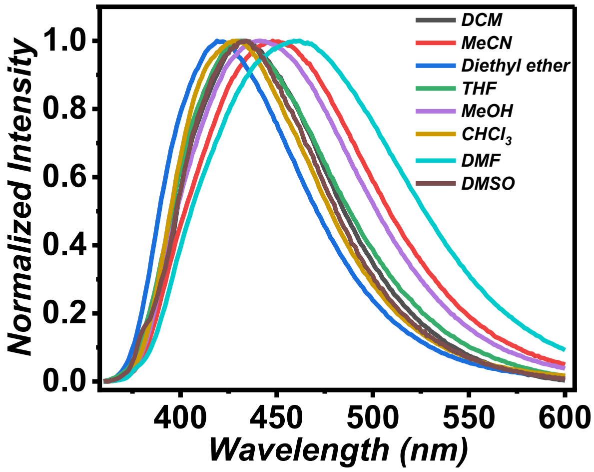

Figure S23. Emission spectra of **1-I** in different solvents (10 μM)

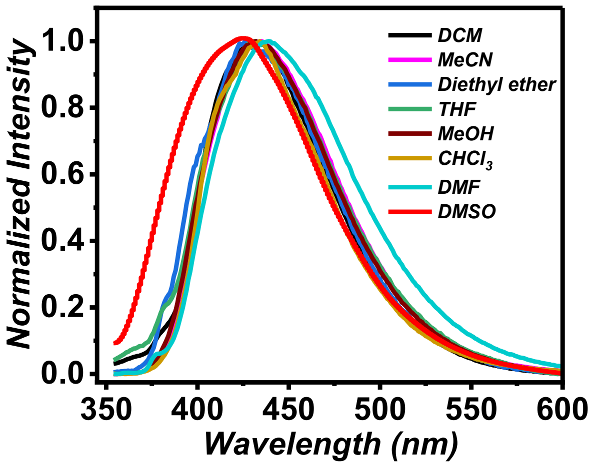

Figure S24. Emission spectra of **2-I** in different solvents (10 μM)

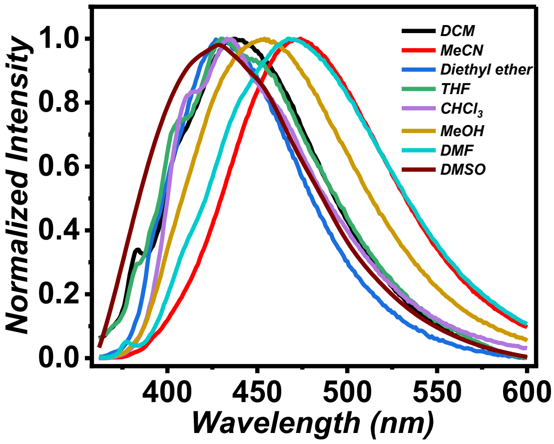

Figure S25. Emission spectra of **3-I** in different solvents (10 μM)

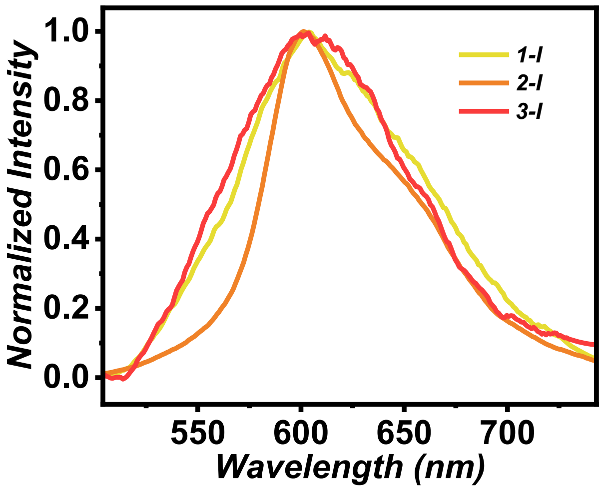

Figure S26. Phosphorescence spectra of **1-I**, **2-I**, and **3-I** in solid-state at room temperature (293 K) under air

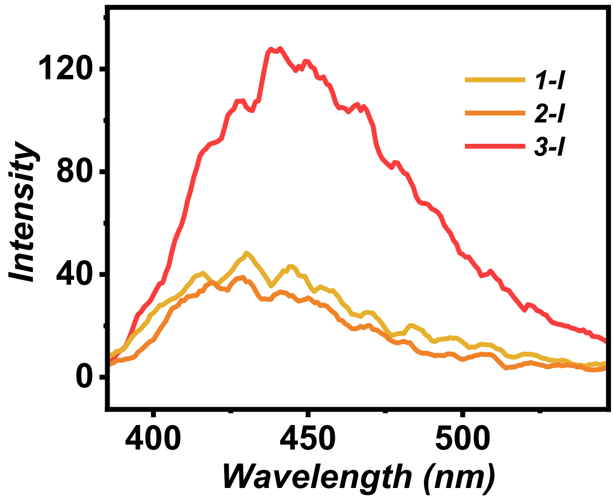

Figure S27. Phosphorescence spectra of **1-I, 2-I,** and **3-I** compounds in dichloromethane under N_2 atmosphere at room temperature (293 K)

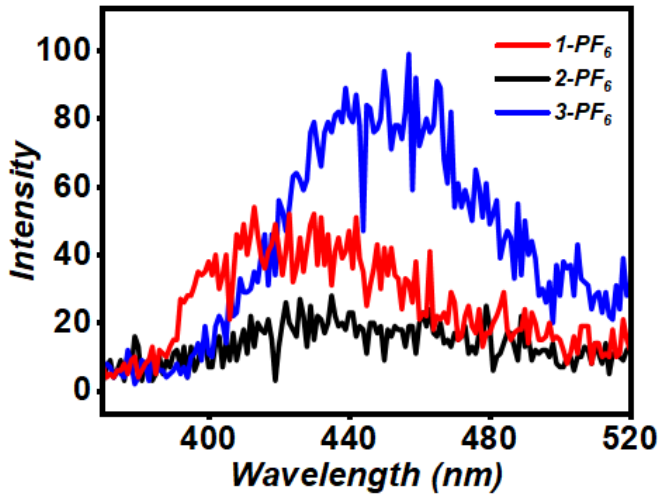

Figure S28. Phosphorescence spectra of **1-PF$_6$, 2-PF$_6$,** and **3-PF$_6$** compounds in dichloromethane at 77 K

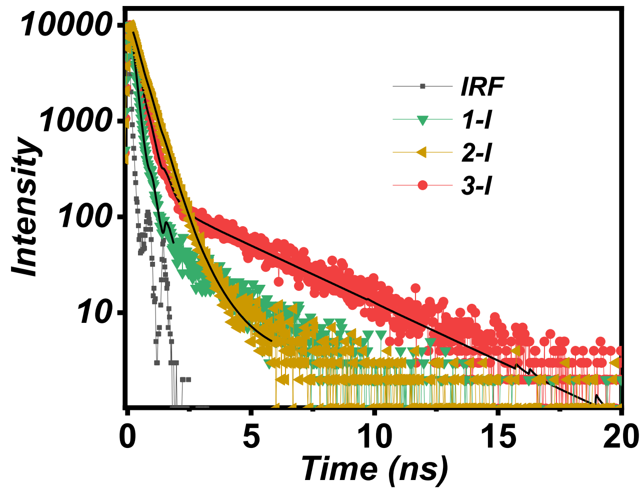

Figure S29. Time-resolved PL decay of **1-I, 2-I,** and **3-I** compounds in dichloromethane at room temperature (τ_{avg}: **1-I** = 0.158 ns, **2-I** = 0.466 ns, **3-I** = 0.748 ns)

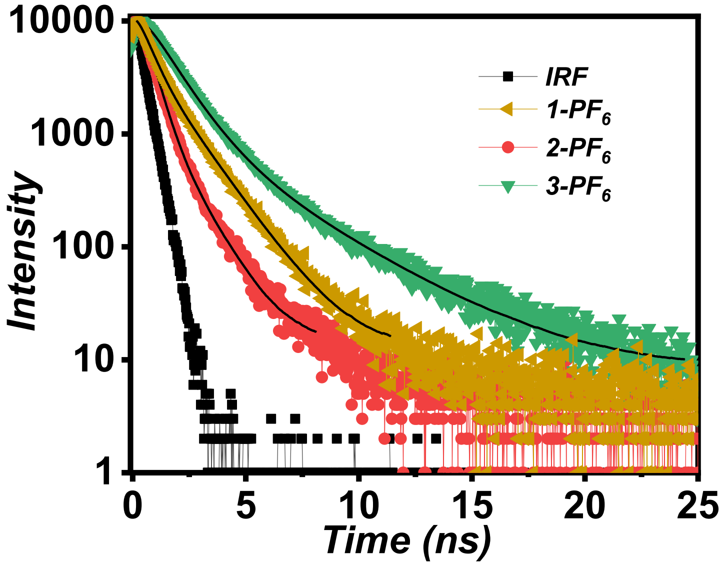

Figure S30. Time-resolved PL decay of **1-PF_6, 2-PF_6, and 3-PF_6** in solid-state at room temperature (τ_{avg}: **1-PF_6** = 0.99 ns, **2-PF_6** = 0.55 ns, and **3-PF_6** = 1.74 ns)

7. Powder XRD analysis

Powder samples of the compounds were obtained by precipitating the column-isolated compounds from their DCM solution by addition of diethyl ether, followed by filtration and drying under vacuum. The powder XRD patterns were simulated using Mercury 2020.3.0 software.

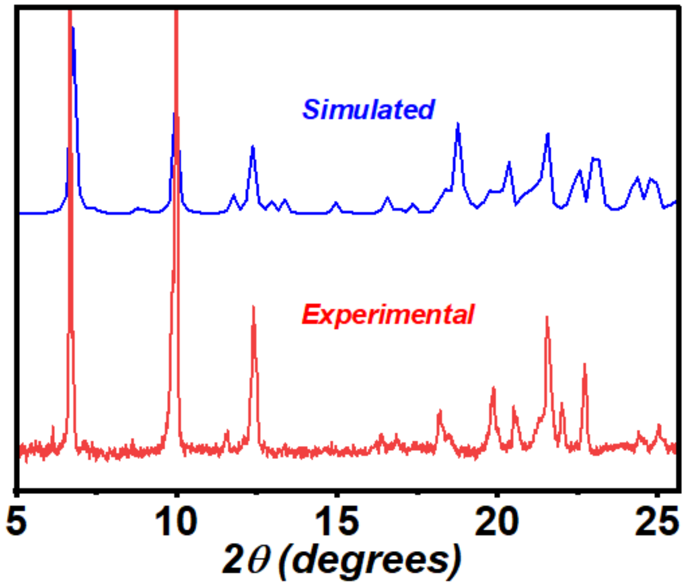

Figure S31: Simulated and experimental powder XRD of **1-I**

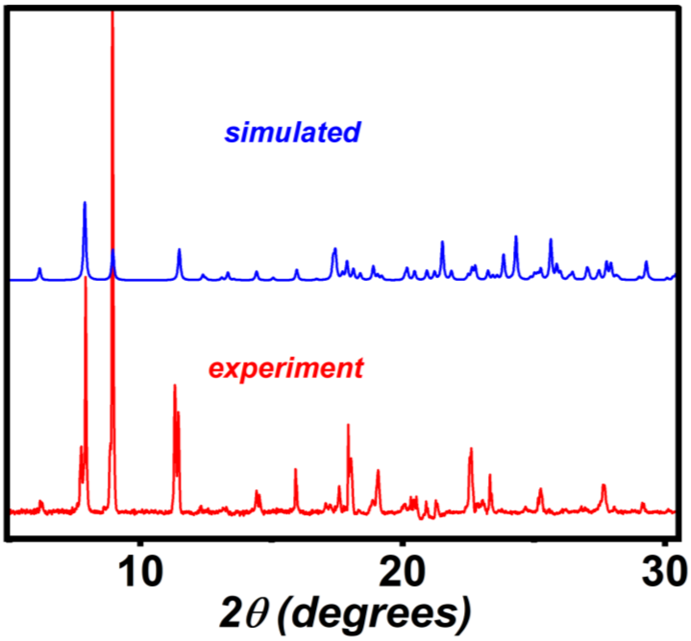

Figure S32: Simulated and experimental powder XRD of **2-I**

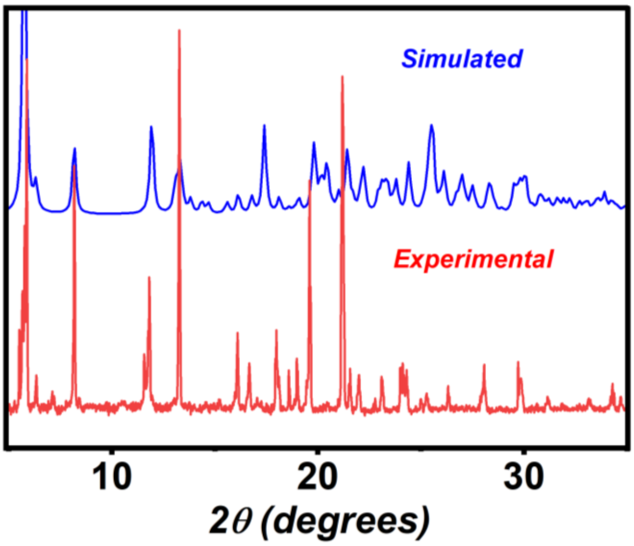

Figure S33. Simulated and experimental powder XRD of **3-I**

8. Single crystal X-ray diffraction studies

General comments. Single-crystal X-ray diffraction data were collected at low temperature (at 140 K or 120 K) using a Bruker D8 QUEST PHOTON 100 diffractometer equipped with graphite-monochromated Mo Kα radiation (λ = 0.71073 Å). Data reduction was performed using the Bruker Apex V software suite. All structures were refined by the full-matrix least-squares method using ShelXL 2018 present in the Olex2 interface. All non-hydrogen atoms were refined anisotropically, and all hydrogen atoms were positioned geometrically and refined using a riding model. The crystal image was made by using the Mercury 2020.3.0 program. The details of the crystal data were provided in the CIF files.

Structural and refinement details. In the crystal structure of **1I** (CCDC No. 2502118), the counteranion 'I' exhibited disorder. The disorder was treated via the PART and EADP instructions. Solvent mask was used in **1I** for dichloromethane. Also, the two-domain twin in **3I** was treated using TWIN/BASF.

Table S1. Crystal data and structure refinement information for **1-I**	
Identification code	**1I**
CCDC No.	2502118
Empirical formula	$C_{35}H_{24}INO$
Formula weight	601.45
Temperature/K	140.00
Crystal system	monoclinic
Space group	C2/c
a/Å	25.9967(13)
b/Å	13.2800(5)
c/Å	17.7015(8)
α/°	90
β/°	93.282(2)
γ/°	90
Volume/Å^3	6101.2(5)
Z	8
ρ_{calc}g/cm^3	1.310
μ/mm^{-1}	1.075
F(000)	2416.0
Crystal size/mm^3	0.05 × 0.04 × 0.02
Radiation	MoKα (λ = 0.71073)
2Θ range for data collection/°	4.094 to 58.254
Index ranges	$-35 \leq h \leq 35$, $-18 \leq k \leq 18$, $-24 \leq l \leq 24$
Reflections collected	142817
Independent reflections	8197 [R_{int} = 0.1001, R_{sigma} = 0.0380]
Data/restraints/parameters	8197/0/347
Goodness-of-fit on F^2	1.051
Final R indexes [I>=2σ (I)]	R_1 = 0.0476, wR_2 = 0.1209
Final R indexes [all data]	R_1 = 0.0786, wR_2 = 0.1377
Largest diff. peak/hole / e Å^{-3}	1.44/-0.58

Table S2. Crystal data and structure refinement information for **2-I**	
Identification code	**2I**
CCDC No.	2495460
Empirical formula	$C_{38}H_{29}IN_2O_2$
Formula weight	672.53
Temperature/K	125.00
Crystal system	monoclinic
Space group	$P2_1$
a/Å	14.085(3)
b/Å	7.2681(8)
c/Å	15.308(3)
α/°	90
β/°	97.143(5)
γ/°	90
Volume/Å^3	1554.9(5)
Z	2
ρ_{calc}g/cm^3	1.436
μ/mm^{-1}	1.066
F(000)	680.0
Crystal size/mm^3	0.31 × 0.2 × 0.13
Radiation	Mo Kα (λ = 0.71073)
2Θ range for data collection/°	4.198 to 59.184
Index ranges	$-19 \le h \le 19$, $-10 \le k \le 10$, $-21 \le l \le 21$
Reflections collected	59135
Independent reflections	8699 [R_{int} = 0.0756, R_{sigma} = 0.0543]
Data/restraints/parameters	8699/1/390
Goodness-of-fit on F^2	1.023
Final R indexes [I>=2σ (I)]	R_1 = 0.0372, wR_2 = 0.0699
Final R indexes [all data]	R_1 = 0.0531, wR_2 = 0.0770
Largest diff. peak/hole / e Å^{-3}	0.71/-0.63
Flack parameter	-0.033(11)

Table S3. Crystal data and structure refinement information for **3-I**	
Identification code	**3I**
CCDC No.	2495459
Empirical formula	$C_{36}H_{23}F_3INO$
Formula weight	669.45
Temperature/K	140.00
Crystal system	monoclinic
Space group	$P2_1/n$
a/Å	6.9559(9)
b/Å	28.730(4)
c/Å	14.9096(19)
α/°	90
β/°	96.720(2)
γ/°	90
Volume/Å^3	2959.1(7)
Z	4
ρ_{calc}g/cm^3	1.503
μ/mm^{-1}	1.131
F(000)	1336.0
Crystal size/mm^3	0.2 × 0.15 × 0.09
Radiation	Mo Kα (λ = 0.71073)
2Θ range for data collection/°	3.95 to 51.032
Index ranges	$-8 \leq h \leq 8$, $0 \leq k \leq 34$, $0 \leq l \leq 18$
Reflections collected	5528
Independent reflections	5528 [R_{int} = 0.0000, R_{sigma} = 0.0493]
Data/restraints/parameters	5528/0/380
Goodness-of-fit on F^2	1.043
Final R indexes [I>=2σ (I)]	R_1 = 0.0395, wR_2 = 0.0775
Final R indexes [all data]	R_1 = 0.0549, wR_2 = 0.0828
Largest diff. peak/hole / e Å^{-3}	0.66/-0.41

9. Crystal packing arrangements and non-covalent interactions of 1-I and 2-I

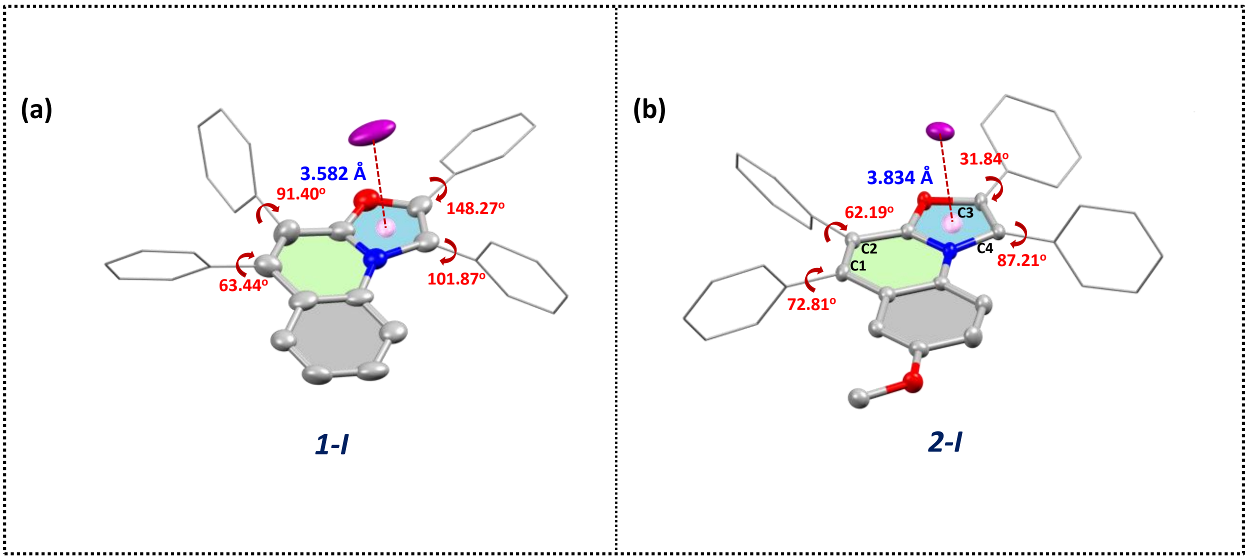

Figure S34. Torsion angles and anion–π^+ interactions with distances for (a) **1-I** and (b) **2-I**

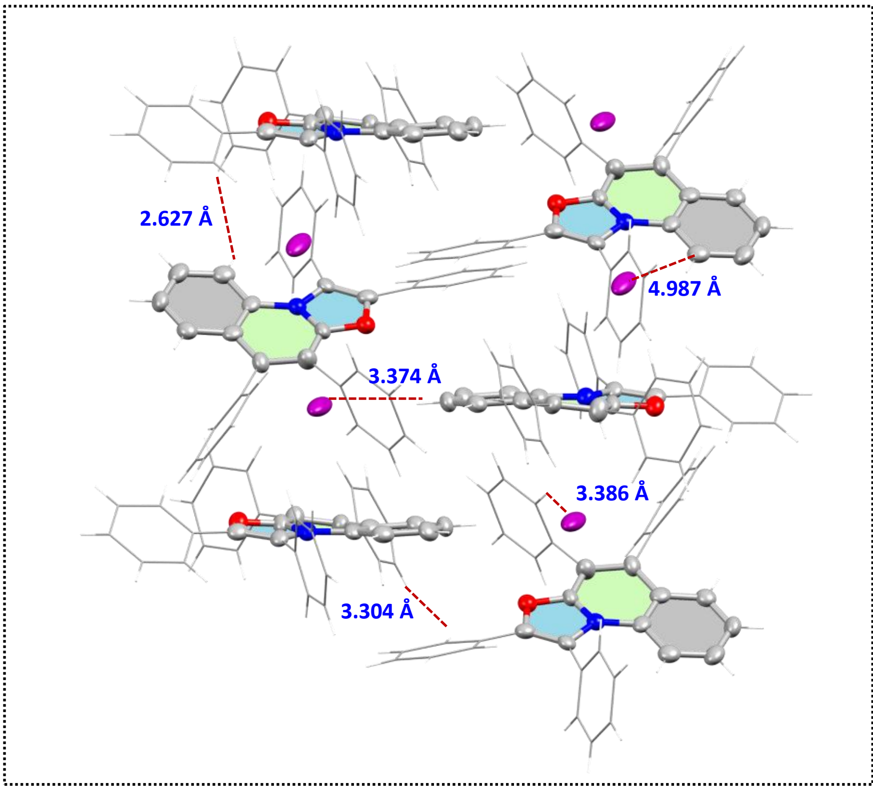

Figure S35. Intramolecular non-covalent interactions in the molecular packing of **1-I**

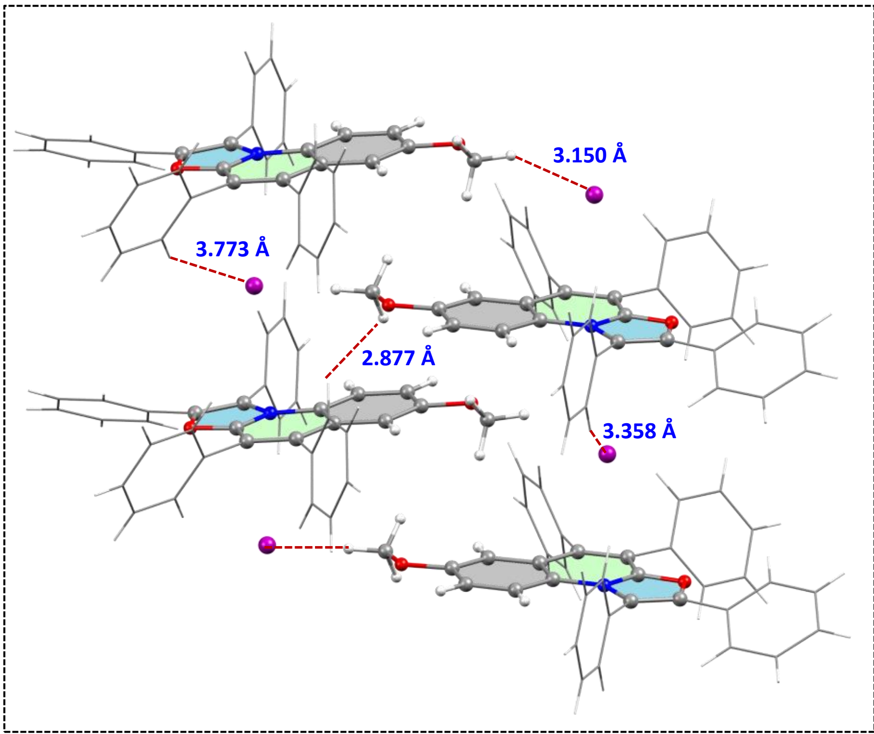

Figure S36. Intramolecular non-covalent interactions in the molecular packing of **2-I**

10. Computational studies

For all of the theoretical studies, the software Gaussian 09 was used. Density functional theory (DFT) simulations were carried out using the LanL2DZ basis set for H, C, N, O and I atoms, as well as the B3LYP exchange-correlation functional. The optimized structure was determined for solvent phase simulations. Frequency calculations were performed to ensure that the optimized structures corresponded to genuine minima. The optimized ground state geometries were discovered to have no imaginary frequency. Images of the highest occupied molecular orbital (HOMO) and lowest unoccupied molecular orbital (LUMO) were acquired from the optimized geometry to investigate electronic distributions and the energy gap between them. Time-dependent (TD)-DFT calculations were carried out on the optimized structure using B3LYP/LanL2DZ as a basis set and CH_2Cl_2 was used as a solvent for calculations (CPCM model). The UV-vis absorption spectra was calculated using the time-dependent DFT. The UV/Vis spectra were simulated using the GaussView5 visualization software package.

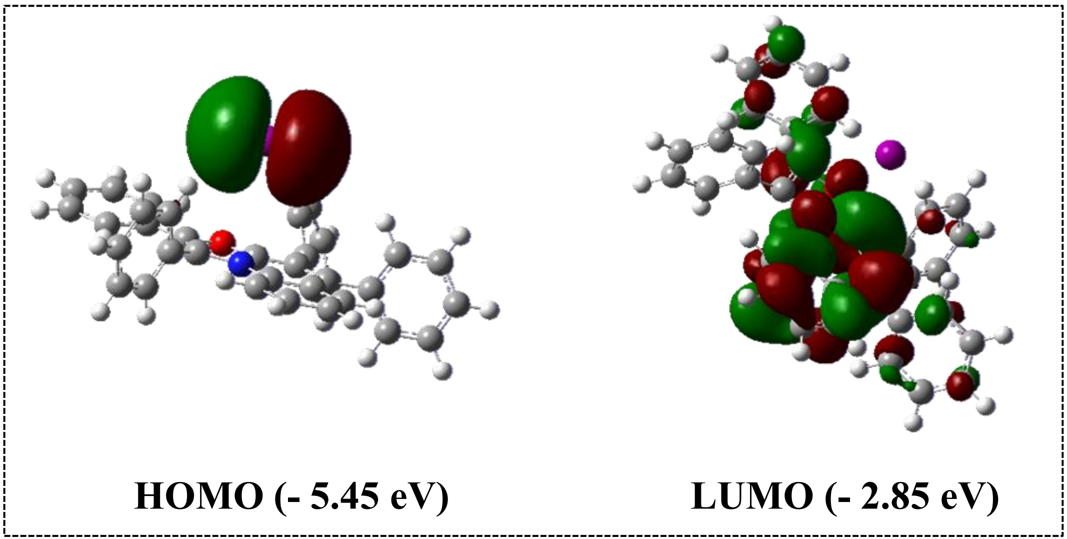

Figure S37. Kohn-Sham frontier orbital representation and MO energies of **1-I**

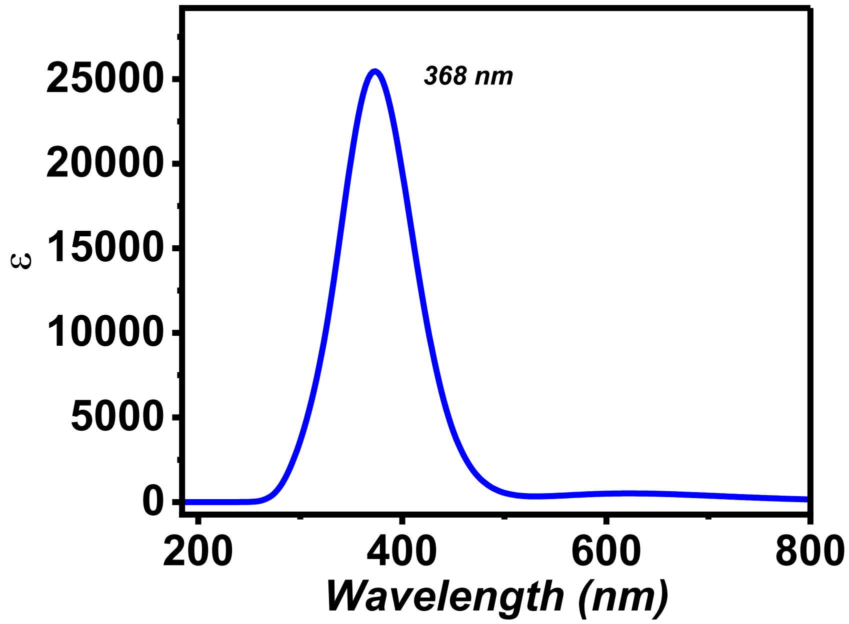

Figure S38. TD-DFT-calculated UV/Vis absorption spectra of **1-I** calculated at B3LYP/LanL2DZ, CPCM-CH_2Cl_2 level of theory

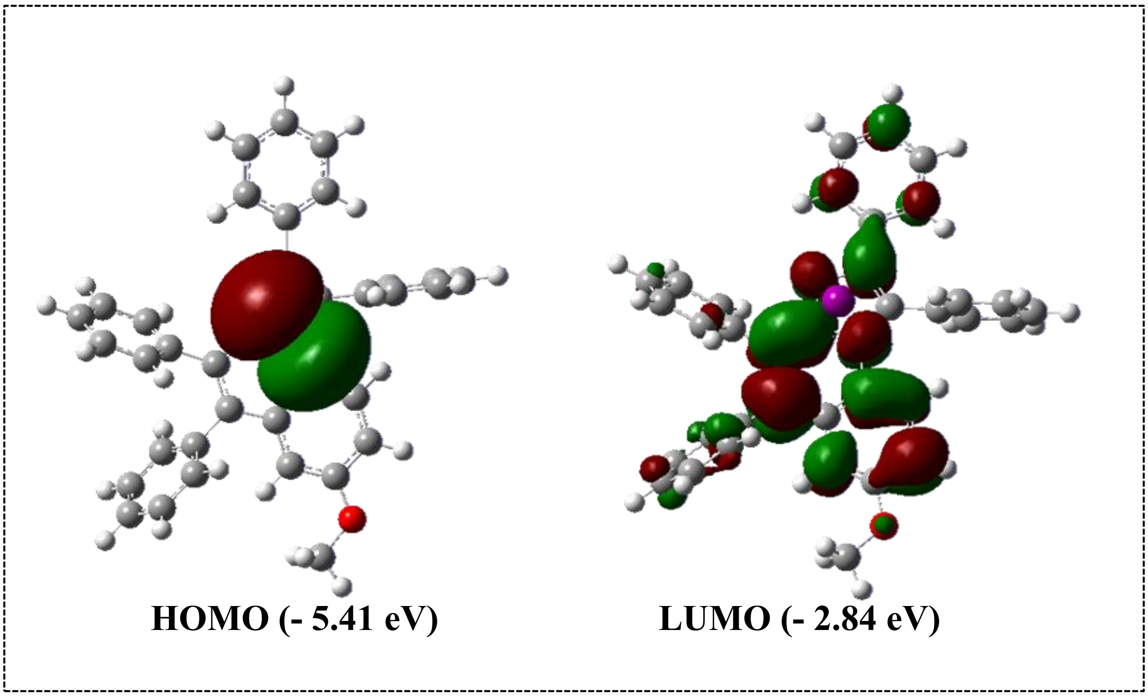

Figure S39. Kohn-Sham frontier orbital representation and MO energies of **2-I**

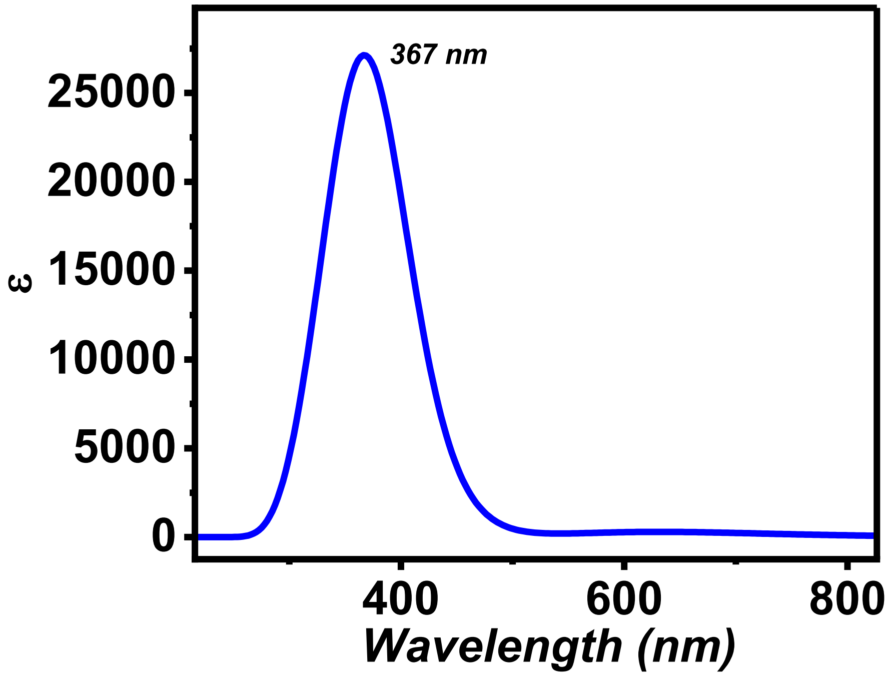

Figure S40. TD-DFT-calculated UV/Vis absorption spectra of **2-I** calculated at B3LYP/LanL2DZ, CPCM-CH_2Cl_2 level of theory

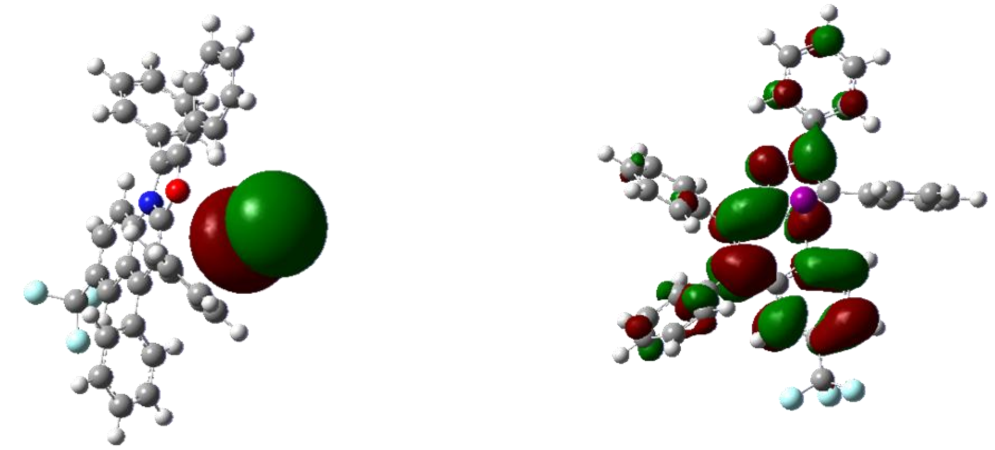

HOMO (- 5.46 eV) LUMO (- 3.10 eV)

Figure S41. Kohn-Sham frontier orbital representation and MO energies of **3-I**

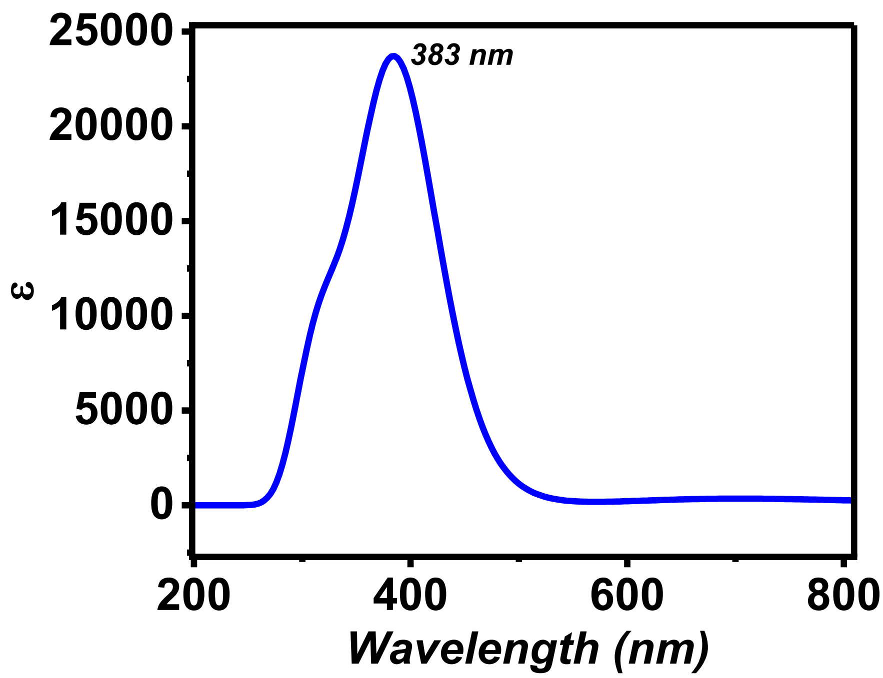

Figure S42. TD-DFT-calculated UV/Vis absorption spectra of **3-I** calculated at B3LYP/LanL2DZ, CPCM-CH_2Cl_2 level of theory

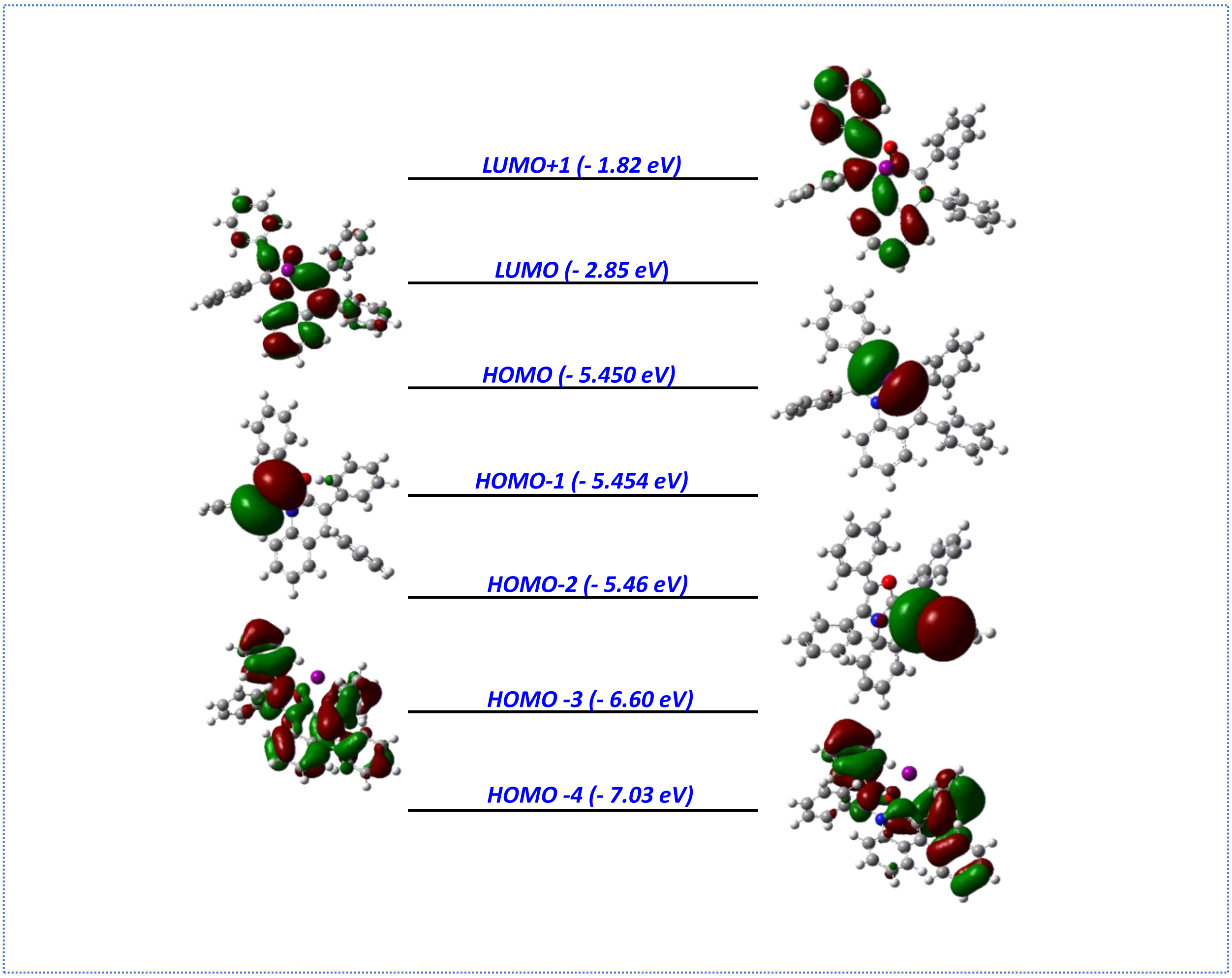

Figure S43. Partial molecular orbital pictures of **1-I**

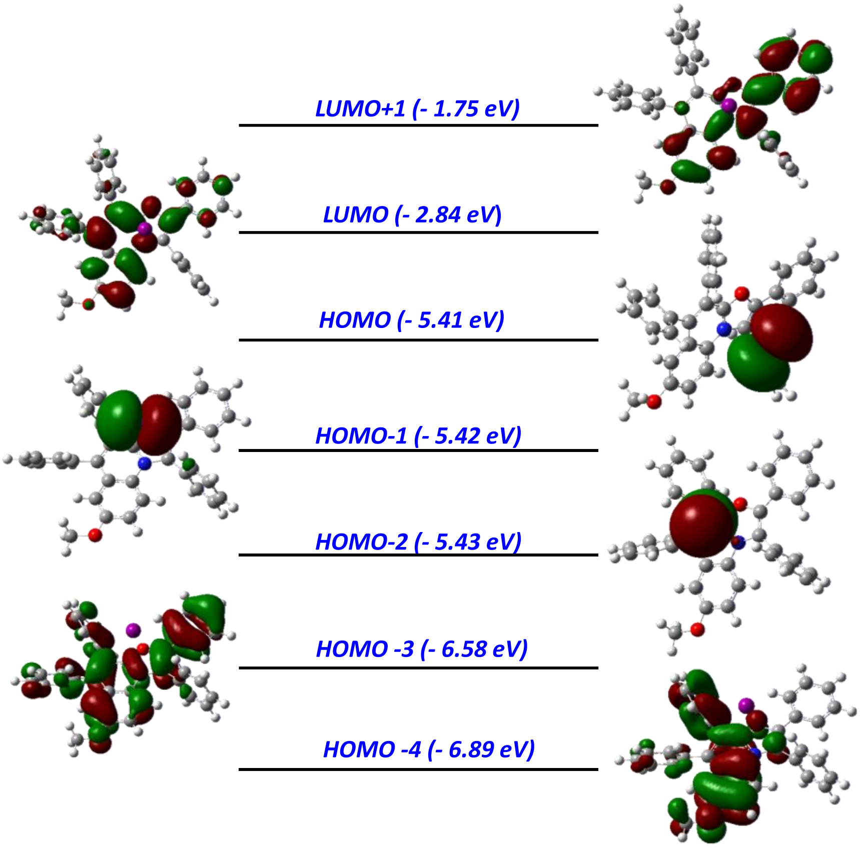

Figure S44. Partial molecular orbital pictures of **2-I**

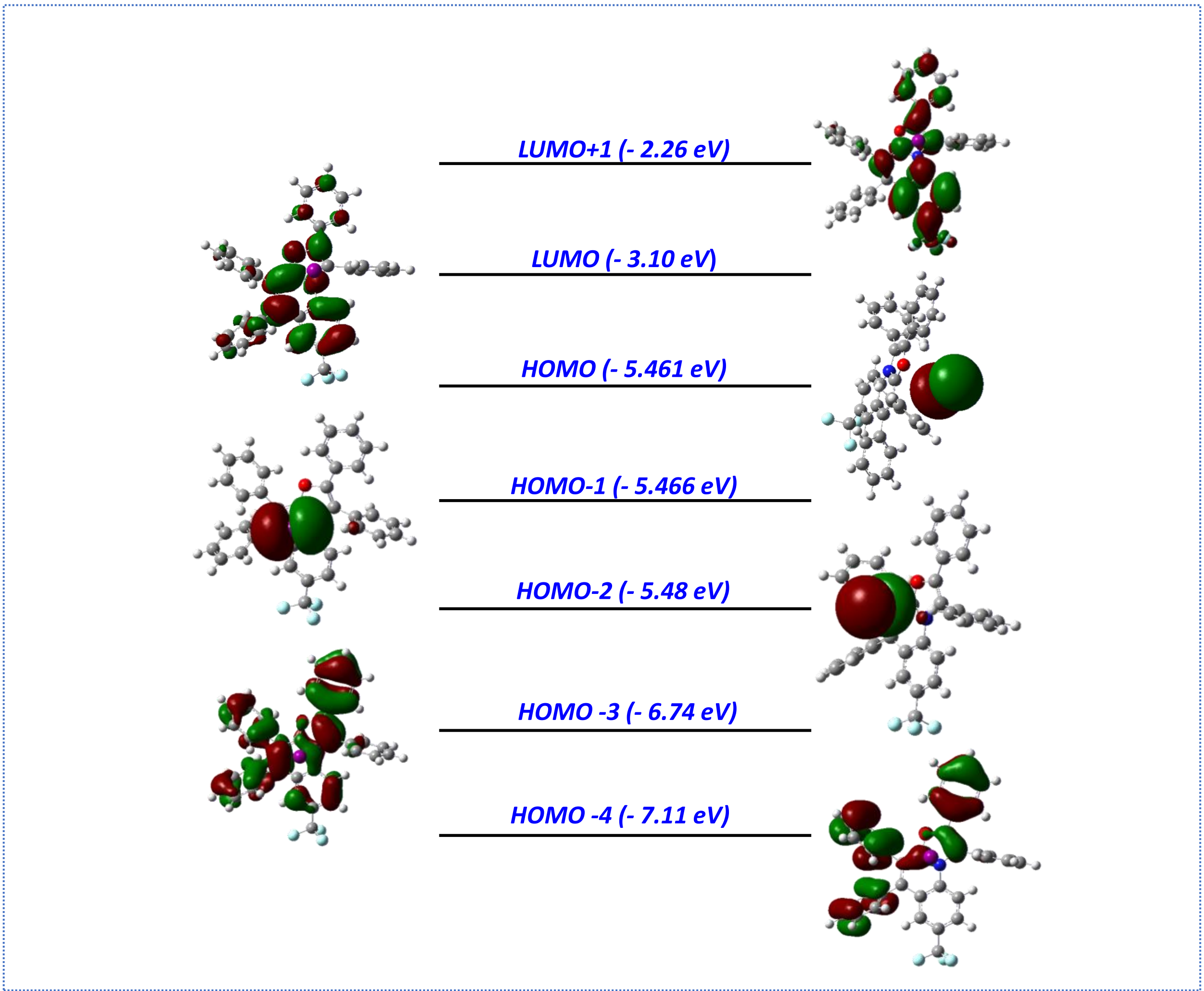

Figure S45. Partial molecular orbital pictures of **3-I**

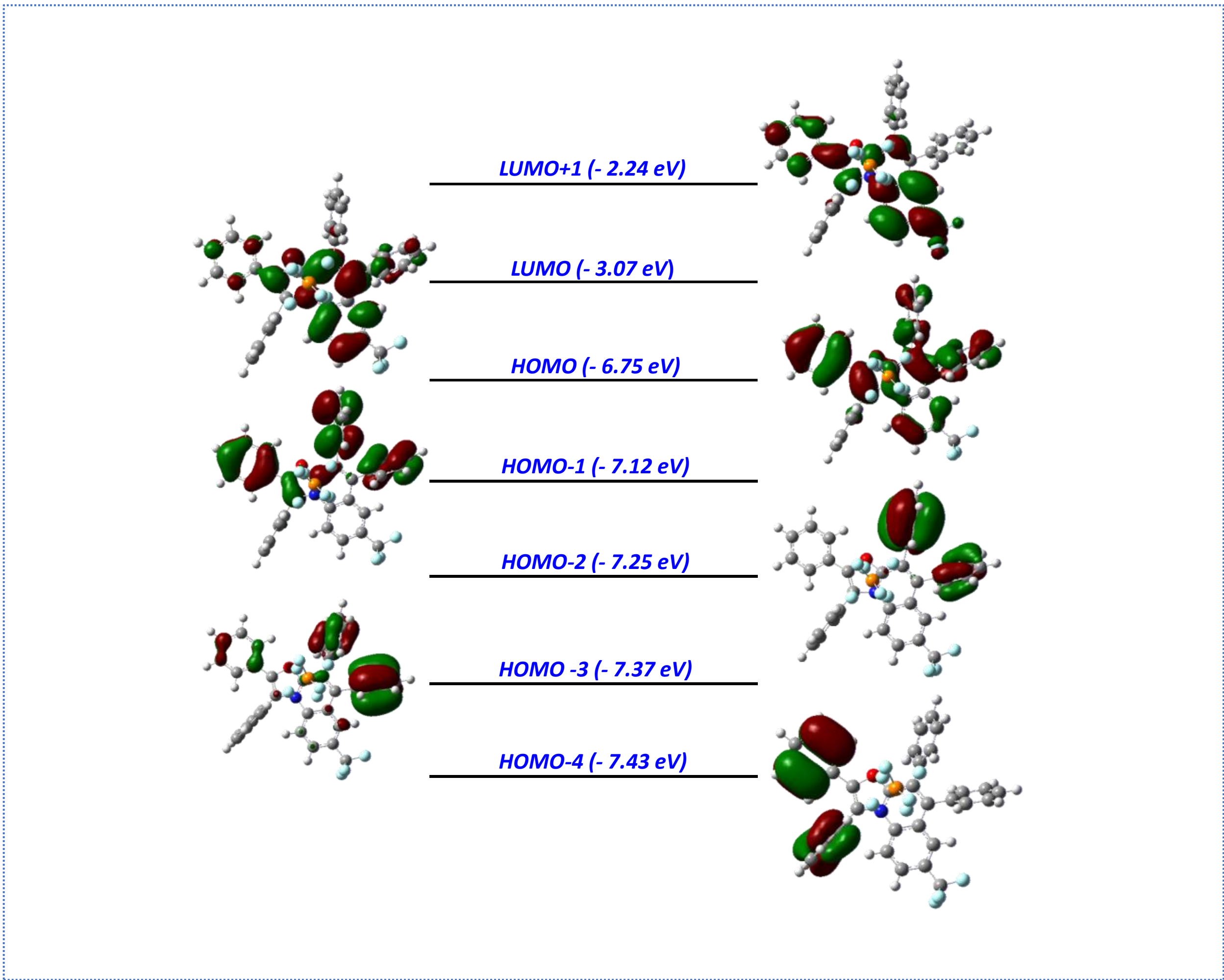

Figure S46. Partial molecular orbital pictures of **3-PF$_6$**

The x, y, and z coordinates for the optimized structures of **1-I**, **2-I, 3-I**, and **3-PF_6** are as below.

1-I

Symbolic Z-matrix:

Charge = 0 Multiplicity = 1

I	3.4368	8.4547	16.556
O	4.2638	4.9911	15.6931
C	3.795	4.98	19.2434
N	2.4196	5.0159	16.874
C	0.6151	5.0111	15.0011
C	0.2198	5.0318	18.0291
C	-0.456	5.018	19.2151
C	0.2746	5.0049	20.4345
C	4.2551	4.8427	10.7099
H	4.5063	4.8014	9.8146
C	5.1641	5.0566	11.6901
H	6.0565	5.1808	11.456
C	4.812	5.098	13.015
H	5.4663	5.2498	13.6607
C	3.511	4.9269	13.3983
C	3.1685	4.978	14.8133
C	3.744	5.0207	16.892
C	4.5165	4.9835	18.1191
C	4.5057	4.9807	20.5991
C	4.775	6.25	21.0802
H	4.7491	7.0434	20.6017
C	5.1461	6.0638	22.6547
H	5.9092	6.6295	22.8579
C	5.4368	4.7807	23.0406
H	6.0605	4.6979	23.7378
C	2.0379	4.9766	15.5027
C	0.0024	6.2107	14.7335
H	0.4803	7.0061	14.8056

C	-1.3285	6.2293	14.3528
H	-1.7403	7.0503	14.1958
C	-2.0527	5.0876	14.2036
H	-2.9524	5.1118	13.9746
C	-1.4038	3.9114	14.4017
H	-1.8679	3.1181	14.255
C	-0.0586	3.8356	14.8261
H	0.3543	3.0167	14.9779
C	1.6798	5.0111	18.0702
C	1.6419	5.0125	20.4396
H	2.0928	5.0304	21.2526
C	2.363	4.9931	19.2768
C	5.9927	4.9855	17.9133
C	6.6501	6.05	17.3628
H	6.1708	6.8088	17.1287
C	8.0066	6.0086	17.1544
H	8.412	6.7122	16.699
C	8.7783	4.9738	17.5892
H	9.7048	4.9876	17.5043
C	8.1206	3.8839	18.1654
H	8.6134	3.1595	18.4793
C	6.7577	3.8701	18.2683
H	6.3299	3.1043	18.5822
C	5.0446	3.8356	22.629
H	4.992	3.0905	23.1872
C	4.5845	3.6907	21.2089
H	4.3826	2.8836	20.7895
C	2.5731	4.7807	12.4207
H	1.6706	4.7393	12.6471
C	2.9564	4.691	11.0907
H	2.3104	4.5185	10.4449
H	-0.25458	4.98882	21.36435

H	-1.52594	5.01705	19.22679
H	-0.30457	5.05704	17.09674

2-I

Symbolic Z-matrix:

Charge = 0 Multiplicity = 1

I	9.8708	-0.435	11.1477
O	6.9152	2.7517	6.2229
O	10.1677	3.3433	13.0361
N	9.9116	3.1871	10.8632
C	12.9855	2.0031	9.7849
C	12.3988	3.2154	10.1198
C	5.4855	2.8011	6.2762
C	7.8927	3.1863	12.2428
C	7.1426	3.0751	11.1085
C	7.7693	3.0126	9.8119
C	6.9921	2.9116	8.6316
C	7.388	3.2765	13.6367
C	11.3085	3.267	11.1136
C	9.2896	3.2452	12.0394
C	9.1722	3.0519	9.6834
C	5.6452	3.0417	11.1879
C	13.9905	4.3398	8.7338
C	14.6064	3.7583	15.2272
C	7.5904	2.8433	7.4066
C	13.4528	3.0831	15.5735
C	12.4168	2.9632	14.675
C	14.7379	4.2816	13.9528
C	9.769	2.9865	8.4197
C	8.9956	2.8745	7.2986
C	11.4261	3.376	12.4539
C	7.2222	4.4619	15.7284

C	4.9634	4.2119	11.4876
C	6.6576	2.2284	14.1867
C	14.5753	3.1384	8.4118
C	2.8832	3.0562	11.1717
C	6.5014	3.4211	16.254
C	6.2206	2.3011	15.5051
C	7.6728	4.3972	14.4145
C	12.5404	3.504	13.392
C	3.5622	4.2082	11.4633
C	14.0769	1.9784	8.9328
C	3.5633	1.8992	10.8922
C	12.9	4.3972	9.5905
C	4.9436	1.889	10.9043
C	13.7056	4.1646	13.0308
H	9.4055	2.8164	6.4437
H	10.7152	3.0206	8.3405
H	6.0443	2.8913	8.6935
H	5.4108	1.0837	10.716
H	3.0842	1.104	10.6917
H	1.9336	3.0584	11.1625
H	3.0826	5.007	11.6486
H	5.4389	5.0041	11.7063
H	8.1738	5.116	14.047
H	7.4148	5.2258	16.26
H	6.1905	3.4734	17.1501
H	5.7305	1.5815	15.8864
H	6.4573	1.4623	13.6612
H	12.5032	5.2316	9.8122
H	14.3382	5.1429	8.3647
H	15.3244	3.1151	7.8279
H	14.4825	1.1484	8.708

H	12.6396	1.192	10.1403
H	13.7963	4.5346	12.1605
H	15.542	4.725	13.7067
H	15.3073	3.863	15.8606
H	13.3736	2.6986	16.4385
H	11.6189	2.5126	14.9266
H	5.1213	2.6965	5.3724
H	5.1544	2.0779	6.8503
H	5.2016	3.6646	6.6422

3-I

Symbolic Z-matrix:

Charge = 0 Multiplicity = 1

I	3.1844	19.8292	12.9899
F	1.1653	18.6831	5.3883
O	-0.3273	19.9444	13.5989
F	-0.4439	17.4133	5.8044
F	1.544	16.8071	6.2886
N	-0.0832	20.0679	11.4267
C	0.3325	18.1746	10.0245
C	-0.7514	22.622	16.6906
H	-0.9211	22.2994	17.5674
C	-0.6912	21.7256	15.6423
H	-0.8297	20.7979	15.7917
C	-0.1983	19.2319	12.4573
C	0.9824	16.4853	14.2312
H	1.8301	16.6282	13.8274
C	0.1727	20.3811	8.9954
H	0.0486	21.3191	9.0777
C	0.887	15.7124	15.3832
H	1.6658	15.3315	15.7726
C	-0.1374	17.0455	13.6759

C	0.1369	19.5709	10.137
C	-0.0326	22.6019	11.098
C	1.2343	23.0616	10.8063
H	1.999	22.6563	11.1979
C	0.537	18.4533	7.6509
C	-0.2673	23.573	14.1527
H	-0.1156	23.9117	13.2778
C	-0.3349	24.4435	15.2395
H	-0.2151	25.3755	15.1011
C	-0.1764	21.3924	11.9227
C	-0.3209	21.2688	13.2495
C	-0.4236	22.2112	14.357
C	-0.0323	17.8471	12.4054
C	0.4922	17.646	8.751
H	0.5715	16.7045	8.6428
C	-0.9982	24.2539	9.6469
H	-1.7572	24.6692	9.2521
C	0.5378	15.8733	11.0387
C	0.3831	19.8323	7.7708
H	0.4257	20.3881	7.0004
C	-1.1525	23.2023	10.5309
H	-2.0216	22.8875	10.749
C	0.2753	24.6934	9.3463
H	0.3878	25.4035	8.7239
C	-0.3406	15.5056	15.9488
H	-0.4192	14.9641	16.7252
C	0.2551	17.3386	11.1942
C	0.7005	17.8385	6.299
C	1.3721	24.1361	9.9208
H	2.2363	24.4749	9.7209
C	-1.3718	16.8588	14.2756

H	-2.1488	17.2666	13.9099
C	-0.5712	23.9752	16.4952
H	-0.6108	24.5758	17.2312
C	-0.4432	14.931	11.2179
H	-1.3108	15.2134	11.4811
C	-1.4618	16.0831	15.3995
H	-2.3089	15.9403	15.8053
C	1.7976	15.4596	10.6834
H	2.4891	16.1003	10.5677
C	2.0749	14.0978	10.4909
H	2.948	13.8105	10.262
C	-0.207	13.5749	11.0254
H	-0.8967	12.9356	11.1569
C	1.056	13.1813	10.6375
H	1.2309	12.2638	10.469

3-PF_6

Symbolic Z-matrix:

Charge = 0 Multiplicity = 1

P	4.9305	12.7818	12.6461
F	4.847	12.7352	11.0522
F	4.4132	14.2767	12.6203
F	3.4267	12.2653	12.723
F	5.0116	12.8161	14.2332
F	6.4244	13.2902	12.548
F	5.4394	11.2727	12.6664
O	6.3393	12.6751	8.2053
F	6.8925	5.055	11.3621
N	5.7872	10.7842	9.1496
F	6.1385	5.9062	13.1192
F	8.1747	6.1251	12.6723
C	6.7361	11.7188	9.0329

C	7.942	11.7668	9.7485
C	6.0246	9.6372	9.9151
C	3.385	10.4818	8.2606
C	8.1561	10.7364	10.6256
C	4.6733	11.1983	8.3603
C	5.4639	7.4408	10.6519
H	4.8679	6.7021	10.6655
C	4.4515	13.2741	6.8295
C	5.0523	12.3504	7.782
C	5.1523	8.553	9.9273
H	4.3425	8.5872	9.4323
C	8.8296	12.9342	9.5413
C	7.2316	9.6214	10.6617
C	6.6651	7.3847	11.3795
C	3.0759	13.3671	6.695
H	2.5065	12.8264	7.2297
C	3.3501	15.04	4.9973
H	2.9727	15.6403	4.3655
C	7.5192	8.4517	11.3862
H	8.3225	8.4018	11.8898
C	9.2172	13.7564	10.6018
H	8.917	13.5651	11.4832
C	2.4855	10.526	9.3115
H	2.6965	11.0087	10.1027
C	9.3164	10.781	11.5645
C	2.5341	14.255	5.7728
H	1.5906	14.3192	5.6782
C	6.9763	6.1269	12.1304
C	3.0787	9.7727	7.1038
H	3.6957	9.7413	6.3825
C	9.2645	13.2477	8.2575

H	8.9973	12.7099	7.5214
C	10.4705	15.1399	9.1082
H	11.0345	15.8901	8.9608
C	10.0329	14.8433	10.377
H	10.2959	15.3935	11.106
C	9.079	10.8706	12.9257
H	8.1871	10.8218	13.2497
C	10.0875	14.3426	8.0485
H	10.3902	14.546	7.1707
C	5.279	14.0729	6.0479
H	6.2233	14.0142	6.1379
C	4.7203	14.9555	5.1358
H	5.2838	15.5054	4.6042
C	0.9767	9.1512	8.0562
H	0.1508	8.6868	7.9914
C	1.278	9.8622	9.201
H	0.6527	9.8961	9.9156
C	10.6277	10.8196	11.1016
H	10.8103	10.7405	10.1734
C	10.1275	11.0319	13.8243
H	9.9516	11.1099	14.754
C	1.8645	9.1129	7.016
H	1.6471	8.6301	6.2263
C	11.6826	10.9766	12.0195
H	12.5811	11.0118	11.7101
C	11.416	11.0792	13.3632
H	12.132	11.1835	13.9775

11. References

S1 Y. Du, T. K. Hyster, and T. Rovi, *Chem. Commun.,* 2011, **47**, 12074-12076